FACULDADE DE ENGENHARIA DA UNIVERSIDADE DO PORTO

# Micro-Hydropower Generation

**Tiago Marques de Almeida**

U. PORTO

FEUP FACULDADE DE ENGENHARIA UNIVERSIDADE DO PORTO

Mestrado em Engenharia Eletrotécnica e de Computadores

Supervisor: Carlos João Rodrigues Costa Ramos

Second Supervisor: Paulo Jorge Campos Costa

July 22, 2024

# Abstract

Taking into consideration the planet's situation regarding climate change, it is important to acknowledge that it may be necessary to take some actions in order to reduce all the problems that result from that.

Starting with the main responsibility for the climate situation, human beings, by exhausting harvesting of all the planet's resources without considering their consequent recycling and reuse, many problems have arrived.

One of the main sources harvested is fossil fuels to produce electricity that nowadays is so necessary for almost every task that is done, from a simple email being sent to the biggest machine being operated.

One of the ways to bypass the previously mentioned problem is to produce electricity more sustainably. For that, many green sources have been explored, such as wind energy, solar energy, bio-energy, geothermal energy and hydropower.

This dissertation explores the implementation of a plug-and-play solution for small hydropower plants specifically designed to utilize places with low water drops to generate energy.

This plug-and-play solution was conceived and designed to electrify specific pathways along the rivers commonly found in Portugal. It enables energy production and storage, ensuring that energy is available during periods of high demand.

This dissertation initially presents a state-of-the-art review, followed by the development of a high-level control system for managing the power plant and battery charging. Subsequently, the sizing and control of a buck-boost converter for connecting the DC bus to the batteries are conducted. This is followed by the sizing and control of the grid converter, implementation of scalar control of the motor. The dissertation also includes the sizing of the turbine and a study of a complementary system.

In the end, it was possible to achieve a viable solution where all systems were successfully simulated, demonstrating the feasibility of the proposed micro-hydropower station. The study concluded that, in this scenario, integrating a photovoltaic system would be advantageous, enhancing the overall energy generation and stability of the power supply.

***Keywords:*** Hydropower plant, renewable energy, buck-boost converter, battery, grid converter, scalar control, photovoltaic system.

# Resumo

Tendo em consideração a situação do planeta em relação às alterações climáticas, é importante reconhecer que pode ser necessário tomar algumas ações para reduzir todos os problemas que resultam dessa situação.

Começando com o principal responsabel pela situação climática, o ser humano, ao explorar exaustivamente todos os recursos do planeta sem considerar a sua consequente reciclagem e reutilização, muitos problemas têm surgido.

Uma das principais fontes exploradas são os combustíveis fósseis para a produção de eletricidade, que atualmente é tão necessária para quase todas as tarefas realizadas, desde o envio de um simples e-mail até a operação das maiores máquinas.

Uma das formas de contornar o problema anteriormente mencionado é a produção eletricidade de forma mais sustentável. Para isso, muitas fontes verdes têm sido exploradas, como energia eólica, energia solar, bioenergia, energia geotérmica e energia hidrelétrica.

Esta dissertação explora a implementação de uma solução plug-and-play para pequenas centrais hidroelétricas especificamente projetadas para utilizar locais com pequenas quedas de água para gerar energia.

Esta solução plug-and-play foi concebida e projetada para eletrificar passadiços ao longo dos rios, estes são frequentemente encontrados em Portugal. Além de permitir a produção também garante o armazenamento de energia, para que esta esteja disponível durante períodos de alta procura.

Esta dissertação inicialmente apresenta uma revisão do estado da arte, seguida pelo desenvolvimento de um sistema de controlo de alto nível para gerir a central elétrica e o carregamento da bateria. Subsequentemente, é realizado o dimensionamento e controlo de um conversor buck-boost para ligar o barramento DC às baterias. Isto é seguido pelo dimensionamento e controlo do conversor de rede, implementação do controlo escalar do motor. A dissertação também inclui o dimensionamento da turbina e um estudo de um sistema complementar.

No final, foi possível alcançar uma solução viável onde todos os sistemas foram simulados com sucesso, demonstrando a viabilidade da estação micro-hidroelétrica proposta. O estudo concluiu que, neste cenário, a integração de um sistema fotovoltaico seria vantajosa, melhorando a geração geral de energia e a estabilidade do fornecimento de energia.

***Palavras-chave:*** Central hidroelétrica, energia renovável, conversor buck-boost, bateria, conversor de rede, controlo escalar, sistema fotovoltaico.

# Sustainable Development Goals of the United Nations

The Sustainable Development Goals (SDGs) represent a set of 17 global objectives aimed at combating environmental climate change, poverty, mortality, social exclusion, and fostering economic growth. The table below outlines each SDG that this project addresses, the specific targets associated with these goals, the contributions made by this project to support these objectives, and the performance indicators used to measure progress.

Table 1: Goals, Contributions, and Performance Indicators for Sustainable Development Goals

| **SDG** | **Goals** | **Contribution** | **Performance indicators and metrics** |
|---|---|---|---|
| 3 - Ensure healthy lives and promote well-being for all ages | 1 - By 2030, reduce the global maternal mortality ratio to less than 70 per 100,000 live births | A mini hydropower station can provide electricity to remote areas, improving healthcare access and potentially reducing mortality rates. | 3.1.1 Maternal mortality ratio<br>3.1.2 Proportion of births attended by skilled health personnel |
| 7 - Ensure access to affordable, reliable, sustainable and modern energy for all | 2 - By 2030, increase substantially the share of renewable energy in the global energy mix | Hydroelectric power is clean and renewable, emitting no greenhouse gases, thus supporting sustainable energy production. | 7.2.1 Renewable energy share in the total final energy consumption |
| 11 - Make cities and human settlements inclusive, safe, resilient, and sustainable | 1 - By 2030, ensure access for all to adequate, safe, and affordable housing and basic services and upgrade slums | Mini hydropower stations can illuminate roads in remote areas, increasing safety for drivers, and provide a power supply for water pumps, ensuring access to water for households | 11.1.1 Proportion of urban population living in slums, informal settlements or inadequate housing |

# Acknowledgements

The conclusion of this dissertation marks the end of a five-year journey during which I experienced significant personal growth and development. As I prepare to embark on a new chapter, it's important to express gratitude to the individuals who have supported me along this path.

First and foremost, I want to express my heartfelt thanks to my family for their unwavering support and for providing me with the necessary conditions to pursue my studies over the past five years.

I am deeply grateful to my girlfriend for her support and encouragement during the challenging times and for providing much-needed distractions during stressful days.

I want to express my deepest gratitude to my friends from the "Quando quiserem" group, who have supported and worked with me on several projects and assignments.A special thank you to my friend, Fábio Alves, whose expertise and patience have been incredibly valuable, especially during this final phase.

I am also grateful to my supervisors, Professor Carlos Ramos and Paulo Costa, for their invaluable guidance and mentorship throughout this work.

Lastly, I would like to thank FEUP for providing the necessary resources and support to ensure the successful completion of my coursework and dissertation.

Tiago Almeida

*"Water is the driving force of all nature"*

Leonardo da Vinci

# Contents

# List of Figures

# List of Tables

# Abbreviations and Symbols

## List of abbreviations

| | |
|---|---|
| BMS | Battery management system |
| C-BBC | Current dc-link back-to-back converter |
| IGBT | Insulated Gate Bipolar Transistors |
| PLL | Phase-locked loop |
| PWM | Pulse width modulation |
| SDG | Sustainable Development Goals |
| SOC | State of charge |
| V-BBC | Voltage dc-link back-to-back converter |

## List of symbols

| | |
|---|---|
| A | Projected area of the rotor |
| AC | Alternating current |
| B | Blade height |
| C | Capacitor |
| $C_p$ | Power coefficient |
| $D_a$ | Turbine inner diameter |
| $D_n$ | Turbine outer diameter |
| $\delta$ | Diameter number |
| f | Voltage frequency |
| g | Gravity acceleration |
| H | Head |
| $H_u$ | Useful head |
| $I_c$ | Locked rotor current |
| $i_{sd}$ | Current in d-axis |
| $i_{sq}$ | Current in q-axis |
| $L_m$ | Magnetization inductance |
| L | Inductor |
| $\text{Load}_{24h}$ | Total load for one day |
| $\text{Load}_{month}$ | Total load for one month |
| $N$ | System efficiency |
| $n_0$ | Nominal speed |
| $N_s$ | Specific speed |
| Pa | Active power |
| $P_0$ | No load losses |
| $P_1$ | Pressure of the fluid one |
| $P_{converter}$ | Available power at the output of the generator converter |
| $Pn$ | Nominal power |
| $Q$ | Plant discharge |
| $Q_{power}$ | Reactive power |
| $R_1$ | Stator resistance |
| $R_2$ | Rotor resistance |
| $R_m$ | Magnetization resistance |
| $\rho$ | Water density |
| $\sigma$ | Characteristic factor of Kaplan turbine |
| $v$ | Water speed |
| $v_{sd}$ | Voltage in d-axis |
| $v_{sq}$ | Voltage in q-axis |
| $V_0$ | No load voltage |
| $W_{average}$ | Average wind |
| $W_{production}$ | Total wind production |
| $\overline{\forall}$ | Maximum mean annual volume |
| $\overline{E}$ | Mean annual energy production |
| $z_1$ | Height of the fluid above a reference |
| Z | Number of turbine blades |
| $\phi$ | Voltage phase angle |

# Chapter 1

# Introduction

## Framework and Motivations

With the growing demand for electricity and the need to reduce climate change and greenhouse gases, interest in developing and using renewable energies has increased.

Between 1st January and 31st August 2023, renewable energy production in mainland Portugal was 19,255 GWh, which represents 68.2% of total production. Of this, 23% came from hydroelectric sources [1].

Although hydro-power is a green energy, it can cause major environmental impacts in large-scale energy projects. These include alterations to the biodiversity of ecosystems, changes to natural landscapes, reduced water quality, and high installation and removal costs.

The water wheel was the first way to harness the energy of water and was used in Ancient Greece to grind grain. In 1880, electricity was produced for the first time in Wisconsin, United States using a small direct current generator.

Micro-hydroelectric plants are power generation systems that use energy in small watercourses and are classified according to their rated power as described in Table 1.1. They differ from large hydroelectric plants in that they have lower production values. These plants represent a sustainable alternative to meet the growing electricity demand.

Table 1.1: Classification of hydropower plants according to the nominal power [2]

| **Classification** | $P_n$ **(MW)** |
|---|---|
| Small hydroelectric plant | $< 10$ |
| Mini hydroelectric plant | $< 2$ |
| Micro hydroelectric plant | $< 0.5$ |

Micro hydroelectric plants are smaller in scale and have a lower environmental impact, so they are an interesting option for more delicate ecosystems. The main advantages of mini-hydro plants are [3]:

- High efficiency, in the range of 70% to 90%;
- A high capacity factor value of around 50%;
- It is easy to predict energy production, as it varies with rainfall patterns;
- The time of greatest production (winter) corresponds to the time of greatest consumption;
- Reduced daily variations in production compared to other renewable energies;
- The capability to produce energy non-stop 24 hours a day;
- Low environmental impact;
- It is a robust technology, systems can last 50 years or more.

## 1.1 Dissertation Objectives

This work aims to develop a technically and economically viable plug-and-play solution for micro-hydro generation with a power output between 1kW and 5kW. The solution is intended to be implemented in rivers in Portugal to enhance tourism and commerce in certain areas. A micro-hydro plant can make it possible to store energy, power lighting and refrigeration loads, thus supporting local businesses and improving the overall infrastructure in these locations. The aim is to:

- Identify and characterize the minimum requirements for a place to be considered suitable for micro-hydro generation. This objective aims to determine the essential criteria a location must meet to be considered viable for installing a micro-hydro generation system. This may include factors such as water flow, waterfall height, water access, and environmental and economic aspects;
- Characterization of the subsystems: turbine, generator, and electronic converters. The primary objective is to comprehensively comprehend and elucidate the pivotal components of the energy generation system. This entails an in-depth analysis of available turbine technologies feasible for the project's scale, viable generator types within this power range, and various electronic converter options that can be employed;
- Market identification or development of project elements and posterior simulation. This objective aims to identify market components for implementing the developed system. Subsequently, simulations will be conducted to verify alignment with the project plan and ensure feasibility.

## 1.2 Dissertation structure

This dissertation is organized into six chapters. Each chapter delves into a specific aspect of the study, providing a comprehensive understanding of the topic.

In the first chapter, an outline of the dissertation is presented, highlighting the main reasons for proposing this theme and the objectives expected to be achieved by the end.

The second chapter provides a state-of-the-art review, analyzing the components of a hydropower station, including turbine types, generator types, converters needed to connect to the grid, and batteries. A market study is conducted, and the software tools used are analyzed.

In the third chapter, two dissertations are analyzed, contributing to improving this work.

The fourth chapter explains the proposed system, detailing the types of loads, batteries, and control methods for different operational scenarios. Various simulations are conducted at the end of the chapter.

The fifth chapter presents a more extensive study of the individual systems, including the battery converter, grid converter, turbine, and generator. The chapter concludes with an analysis of ways to improve the system.

The final chapter summarizes the conclusions of this work, assesses the achievement of the objectives, and outlines future work.

# Chapter 2

# Background and Fundamental Aspects

## 2.1 Hydro-power basics

Gross head is the total height of the waterfall and can be measured between the lower and upper water levels, this can vary depending on the amount of water stored in the upper level and the flow of water available in the river and power stations can be classified as shown in the table below.

Table 2.1: Classification of hydro-power stations according to gross head [2]

| **Classification** | **H (m)** |
|---|---|
| Low drop | 2-20 |
| Medium fall | 20-150 |
| High fall | >150 |

The discharge from the power station is generally a fraction of the water flowing into the watercourse. It is not desirable to build turbine openings to accommodate the total flow, as this would require huge turbines.

The expected power output of a hydroelectric power station can be calculated using the following expression[4]:

$$P(kW) = \frac{\rho \times g \times Q \times H \times N}{1000} \tag{2.1}$$

Where:

- $\rho$, is the water density;
- g, is the gravity acceleration $(m^2/s)$;
- Q, is the plant discharge $(m^3/s)$;
- H, is the head (m);
- N, is the system efficiency.

In small hydro schemes, it is common to find efficiencies of around 70%.[4] With this simplification, it is possible to have a reference for choosing the turbine-generator set, taking into account the products available on the market.

### 2.1.1 Hydrological study

To determine the amount of energy that can be produced at a given location on a river, it is crucial to know the average flow of water in the river. To do this, two main types of graphs can be used: the Annual Hydrograph and the Mean flow duration.

The Annual Hydrograph, as we can see in the Figure 2.1, is a graph that shows the flow of water as a function of time, usually over a year. This graph makes it possible to visualize the variation in water flow over time, which can be useful for understanding how energy production will be throughout the year.

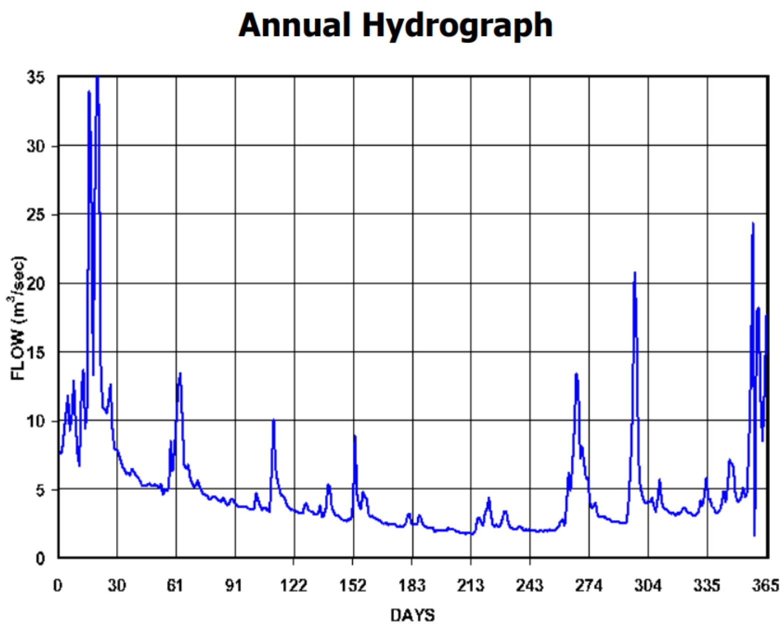


Figure 2.1: Annual Hydrograph [3].

On the other hand, the mean flow duration curve is a graph that shows the mean water flow as a percentage of time as shown in figure 2.2, usually for a year. This graph makes it possible to identify the percentage of the time when the water flow is equal to or greater than a certain value.

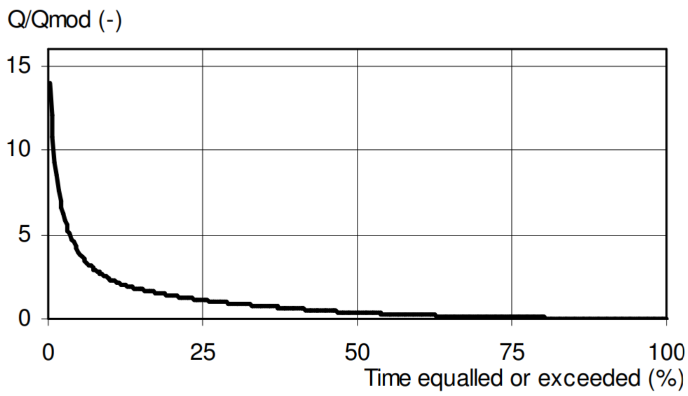


Figure 2.2: Mean flow duration curve [5].

In situations where there is no energy storage, the calculation of the mean amount of energy that can be produced can be carried out as shown in the equation 2.2, in this equation, this equation does not take into account the minimum flow and the reserve flow [5].

$$\overline{E}(GWh) = \frac{\overline{\forall} \times H}{\frac{3600}{g \times N}} \tag{2.2}$$

Where:

- $\overline{\forall}$, is the maximum mean annual volume $(hm^3)$.

## 2.2 Hydro-power schemes

Hydro generation can be made with the following schemes [5]:

- Dam scheme, the dam aims to raise the upstream water level. The powerhouse can be incorporated either downstream or in the interior of the dam;
- Diversion scheme – The utilization of diversion structures, similar as conducts, tunnels or galleries permits the head gain;
- Mixed scheme - A dam can incompletely raise the net head and a hydraulic circuit will raise the other part.

According to the water discharge, they can also be classified as follows [5]:

- Run-of-river scheme, the most common structure in micro-hydro plants, energy is generated without regulating inflows;

- Daily regulation scheme, there is a small reservoir to store the water, and energy is produced according to demand;
- Seasonal regulation scheme, this scheme is usually applied in larger plants, with a reservoir with sufficient capacity to store water from the rainy season to the dry season;
- Cascade scheme, is a standard technique to use the river and maximize the benefits from the river's falls.

## 2.3 Hydro-power constitution

In general, micro-hydro systems are made up of the following elements:

- Intake;
- Feeder canal;
- Forebay;
- Penstock;
- Powerhouse.

### 2.3.1 Intake

Intake, is the most important point in the plant, since it is where the water is collected. It must be chosen correctly so that it is possible to obtain a sufficient flow rate to get good yields from the system and so that it affects the ecosystem as little as possible.

Water can be collected using sand or gravel which, when placed in strategic locations, cause a detour in the flow of water. By analyzing the site, it may be possible to take advantage of its natural characteristics. If they are used, extra care must be taken to avoid damage to the turbines.

In certain situations, it may be necessary to build a small weir to raise, retain, and divert the water. The difference between a weir and a dam is the storage capacity, in a weir the water stored is quite small.

### 2.3.2 Feeder Canal

Feeder canals are channels responsible for transporting water from the reservoir to the loading chamber. They usually have a slight slope and are open, but can also be closed [6].

### 2.3.3 Forebay

The charging chamber is a hydraulic device between the weir and the powerhouse, responsible for protecting the hydraulic circuit from pressure fluctuations and can also act as a water reservoir [6].

### 2.3.4 Pensotck

The penstock is a forced pipe and is an important component in a power station. It transports water from the forebay tank through pipes on steep slopes.

### 2.3.5 Powerhouse

This is the building where the equipment responsible for converting the energy stored in the water into electrical energy will be installed, namely the turbine and generator, batteries, electronic converters, and electrical protection devices can also be found. The size of the powerhouse will depend on the number of generators, turbines, and power installed.

## 2.4 Hydraulic turbines

The hydraulic turbines of a hydroelectric power station are the components responsible for transforming the kinetic and potential energy of water into mechanical energy, later it will generate electricity in the generator. Turbines directly affect the plant's performance, which is why it is essential to choose a turbine that is suitable for the height of the waterfall, the flow rate, and the specific speed of the turbine. Turbines need to be serviced regularly as they suffer a great deal of wear and tear due to the action of the water, which affects their efficiency.

There are two types of turbines, denoted as action and reaction:

- In an action turbine, the water's potential energy is mostly transformed into kinetic energy before it enters the runner, after which the water is at atmospheric pressure;
- In a reaction turbine, the turbine runner is submerged and the pressure variation in the water occurs as it passes through the turbine.

### 2.4.1 Action turbines

Action turbines encompass a range of hydroelectric turbines utilized for converting water's potential energy into kinetic energy. Among these, the Pelton turbine stands out, typically applied in locations with heights exceeding 60 meters.

In these turbines, water is propelled onto a wheel featuring multiple buckets via directed jets aimed precisely at the buckets' interiors and peripheries. The conversion of all potential energy into kinetic energy occurs at the nozzle without the reliance on a draft tube.

A draft tube, in hydroelectric systems, serves as a conduit directing water away from the turbine's outlet to prevent turbulence and facilitate efficient energy transfer. It's a critical component in some turbine designs, but notably absent in Pelton turbines.

Moreover, adjusting the turbine's specific speed can be accomplished by integrating extra nozzles. Regulation of mechanical power involves manipulating the injectors' valve system. Additionally, increased power output can be achieved by interconnecting multiple turbines to a generator.

### 2.4.2 Reaction turbines

The primary variants of reaction turbines encompass the Kaplan and Francis turbines.

Reaction turbines necessitate robust construction to endure elevated pressures due to their direct interaction with the water flow. As water traverses the turbine, it undergoes a reduction in pressure, eventually descending below atmospheric pressure.

### 2.4.3 Low-drop turbines

#### 2.4.3.1 Banki-Mitchell Turbine

It is an action turbine also known as a Cross-Flow turbine, with application in areas of low waterfall. They were invented by Banki and later improved by John Isaac Thornycroft and Allan Robertson Mitchell, their structure can be observed in Figure 2.3.

In the context of Banki turbines, their efficiency remains relatively constant across different water flow rates. This characteristic distinguishes them from some other turbine types. While their overall efficiency might be lower compared to certain turbines, such as the Francis or Kaplan, Banki turbines display an advantage by maintaining a consistent efficiency even when the water flow fluctuates. This attribute makes Banki turbines particularly suitable for installations situated in rivers or locations where water flow rates are variable. [6]

Due to the symmetry of a Banki turbine, its length can theoretically be increased to any size without changing any of its hydraulic characteristics. Thus, doubling the size of the turbine almost doubles the power supplied at the same speed. It is, therefore, clear that the lower the drop, the larger the turbine and that it will become more compact as higher drops are referred to [6].

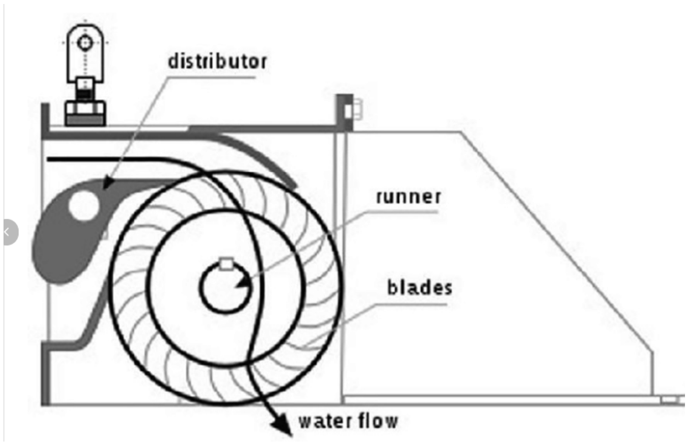


Figure 2.3: Cross flow Turbine [7].

#### 2.4.3.2 Francis Turbine

The distinguishing feature of the Francis turbine lies in its wheel structure, comprising a series of fixed fins forming hydraulic channels. These channels efficiently radially receive water and guide it towards the rotor's outlet in an axial direction. In smaller-scale projects, Francis turbines with a horizontal axis are commonly employed [6].

Adaptable to varying waterfalls and flow rates, the Francis turbine's functionality is governed by a crucial component known as the distributor. This pivotal mechanism effectively controls the volume of water entering the turbine, enabling regulation of power output while maintaining a constant rotational speed. Moreover, the distributor facilitates the closure of the water intake when the plant ceases operations, contributing to the turbine's operational flexibility [6].

We can see an example of a Francis turbine in the figure below.

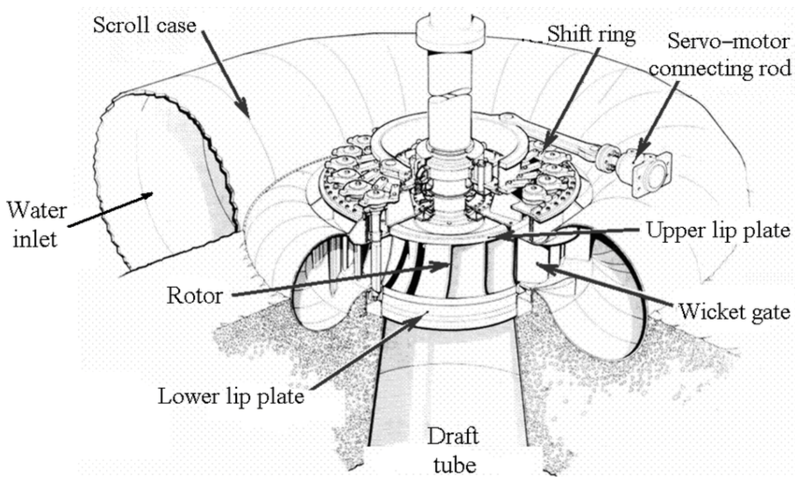


Figure 2.4: Francis turbine [8].

#### 2.4.3.3 Kaplan and propeller turbines

Kaplan-type turbines are composed of either an open or closed inlet chamber, a distributor, and a wheel featuring either a frame or five propeller-shaped blades, as depicted in Figure 2.5. When the turbine blades are adjustable and capable of movement up to 30°, the turbine is referred to as a Kaplan turbine. Conversely, if the blades remain fixed, the turbine is known as a propeller or propeller turbine [6].

When the blades are adjustable, Kaplan-type turbines exhibit versatility, allowing their utilization in scenarios where the water flow ranges from 25% to 125%. This adaptability sets them apart from other turbines operating within a narrower flow range of 40% to 100% [6].

The bulb turbine represents a variant of the propeller turbine design, distinguished by its configuration where the generator is situated at the center of the water passage. This design is particularly effective in scenarios characterized by high water flow and low head.

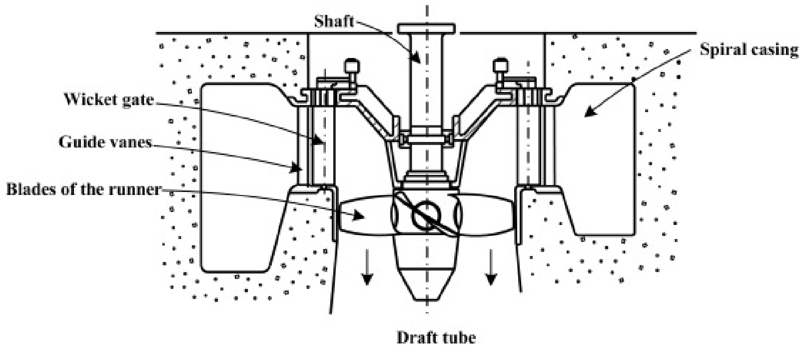


Figure 2.5: Kaplan turbine [9].

#### 2.4.3.4 Choosing the turbine

The selection of a turbine significantly influences a power station's performance, emphasizing the need for a meticulous and precise selection process. Choosing a turbine involves careful consideration of factors such as the head drop, water flow, power requirements, and specific speed.

The specific speed serves as a crucial parameter for comparing hydraulic turbines based on their performance, it is defined as the rotational speed of a turbine of similar size to the one chosen and which would produce 1 kW at a head drop of less than 1 meter. In Figure 2.6, you can see the specific speed as a function of each turbine type, and in the expression below, you can see how it is calculated [5].

$$N_s = 2 \times n_0 \times \frac{\sqrt{\pi \times Q}}{(2 \times g \times H_u)^{0.75}} \tag{2.3}$$

Where:

- $n_0$ is nominal rotational speed $(rpm)$;
- $H_u$ is useful head (m);
- Q, is flow $(m^3/s)$.

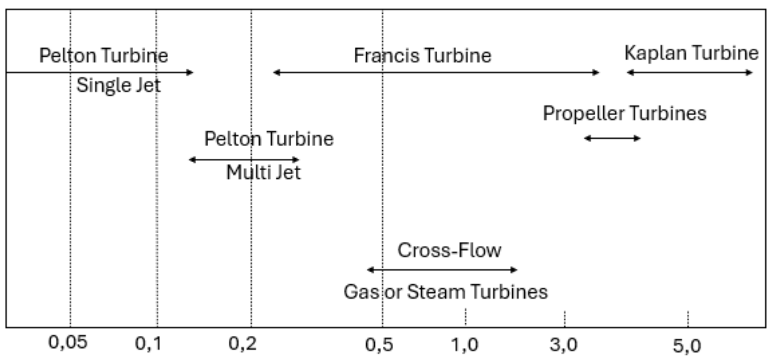


Figure 2.6: Turbine type depending on specific speed [10].

Table 2.2 shows the ideal operating conditions for each type and the nominal power that can be obtained.

Table 2.2: Range of standard turbines [5]

| Type | Hydraulic Turbine | H (m) | Q ($m^3/s$) | P (kW) | Ns (r.p.m) |
|---|---|---|---|---|---|
| **Reaction** | Bulb | 2-10 | 3-40 | 100-250 | 200-450 |
| | Kaplan and propeller - axial flow | 2-20 | 3-50 | 50-5000 | 250-700 |
| | Francis with high specific speed - diagonal flow | 10-40 | 0.7-10 | 100-5000 | 100-250 |
| | Francis with low specific speed - radial flow | 40-200 | 1-20 | 500-15000 | 30-100 |
| **Action** | Pelton | 60-1000 | 0.2-5 | 200-15000 | <30 |
| | Turgo | 30-200 | | 100-6000 | |
| | Banki-Mitchell (Cross-flow) | 2-50 | 0.01-0.12 | 2-15 | |

The efficiency values may vary depending on the turbine manufacturer, but the normal efficiency values are shown in the table below.

Table 2.3: Typical values of efficiency [6]

| Turbine | Efficiency |
|---|---|
| Banki-Mithell (Cross-flow) | 0.8 |
| Kaplan | 0.91 |
| Kaplan with double regulation | 0.93 |
| Francis | 0.94 |

When selecting a turbine, understanding its operating parameters is crucial. Nominal flow typically occurs for a limited duration within the year, and energy production significantly diminishes outside these operating parameters. Table 2.4 displays the diverse operational values specific to each turbine type, providing valuable insights for informed decision-making.

Table 2.4: Operating values for different types of turbines [6]

| Turbine | $\alpha_1 = Qmin/Qn$ | $\alpha_2 = Qmax/QN$ |
|---|---|---|
| Kaplan with rotor regulation | 0.4 | 1 |
| Kaplan with double regulation | 0.25 | 1.25 |
| Francis | 0.35 | 1.15 |
| Propeller | 0.75 | 1 |

## 2.5 Generator

The generator plays a critical role in converting mechanical energy into electrical energy, and its selection depends on various factors such as the turbine type, desired output, budget, and nominal speed.

The realm of electrical generators encompasses two primary classifications: asynchronous and synchronous generators. These distinctions primarily arise from the mode of excitation and the relationship between the magnetic field's speed and the rotor [11].

In asynchronous generators, the magnetic field is induced electromagnetically through the rotation of the stator's magnetic field. The rotor, in turn, operates at a higher speed than the stator's magnetic field. Asynchronous generators, often praised for their cost-effectiveness, durability, and reliability, can be broadly categorized into two types: squirrel-cage and wound-rotor generators [12].

Squirrel-cage generators feature a rotor shaped like a squirrel cage, while wound-rotor generators comprise a rotor wound with wire coils.

Conversely, synchronous generators generate their magnetic field through an external direct current source. In synchronous generators, the rotor's speed synchronizes precisely with the stator's magnetic field. This category includes various types, such as Permanent Magnet Synchronous Motors, Reluctance Synchronous Motors, and Salient-Pole Synchronous Motors.

Permanent Magnet Synchronous Motors utilize permanent magnets to establish the magnetic field, while Reluctance Synchronous Motors feature variable reluctance due to rotor rotation. Salient-Pole Synchronous Motors, on the other hand, leverage salient poles in the rotor to create fluctuations in the magnetic field.

In Portugal, most power stations use synchronous generators and this is due to two reasons [2]:

- Mini hydropower stations began to develop in the 1980s and at that time there was insufficient knowledge of how asynchronous machines work as generators;
- The power stations are essentially low-fall, so the turbine speed is low, and there were no options on the market with motors with a greater number of poles (these were of no use in the industry), so it was obligatory to use speed multipliers.

## 2.6 Grid connection

The connection to the grid can be made via a transformer or via electronic converters however converters have been more widely adopted as they have the following advantages [13]:

- More precise control;
- Flexibility and efficiency;
- Enhanced adaptability.

Although it has some advantages, it also has some disadvantages, namely;

- Complex design;
- Limited overload capacity.

Electronic converters can be used to connect to the power grid, and they can be the following:

- AC-AC converter with DC link;

- Matrix converter;
- Hybrid matrix converter.

### 2.6.1 AC-AC converter with DC link

There are two types of DC link converters:

- The circuit depicted below illustrates a voltage DC-link back-to-back converter;

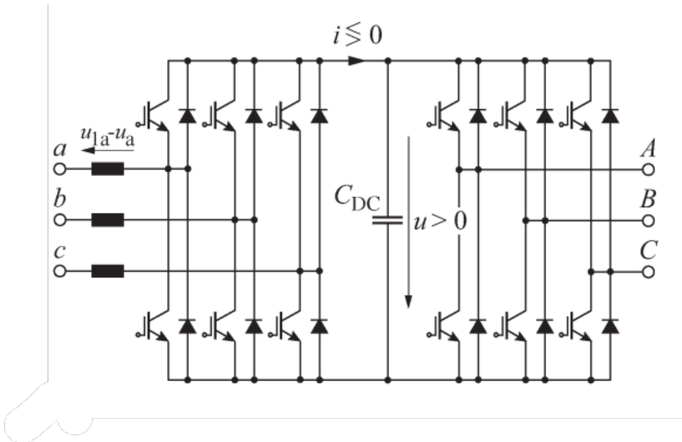


Figure 2.7: V-BBC [14].

- The provided diagram in Figure 2.8 showcases a current DC-link back-to-back converter.

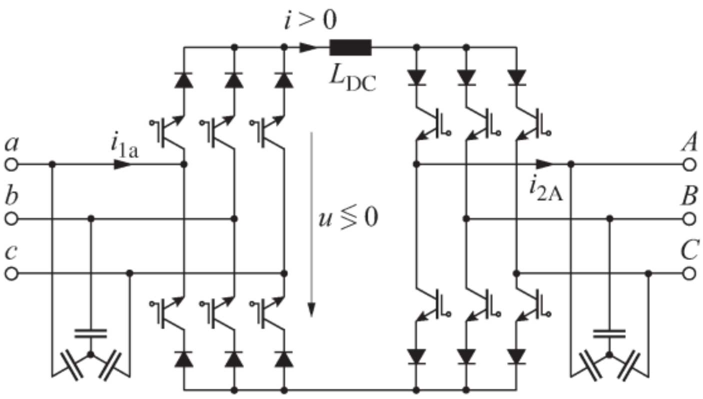


Figure 2.8: C-BBC [14].

The converter can be implemented by connecting a PWM rectifier and a PWM inverter, the dc link will be responsible for storing energy and this link is common to both converters, in the case of a Voltage DC-link back-to-back converter the DC link is a capacitor and in cases where a coil is used it is a Current DC-link back-to-back converter.

To implement the V-BBC, 12 IGBTs and 12 diodes or RC-IGBTs are needed, and for the C-BBC, 12 IGBTs and 12 diodes or RB-IGBTs are needed [14].

The great advantage of having a DC-link is the decoupling of the converter phases and, in addition, having a quantity of input energy independent of the mains results in a higher utilization factor for the converter [14].

One disadvantage of having a DC-link converter is that the component responsible for energy storage (capacitor or coil) is much larger than the rest of the converter's components [14].

### 2.6.2 Matrix converter

Matrix converter is an AC-AC converter, capable of converting energy without relying on a DC link.

Implementing a matrix converter necessitates the use of 18 IGBTs and 18 diodes, as depicted in the figure below [14].

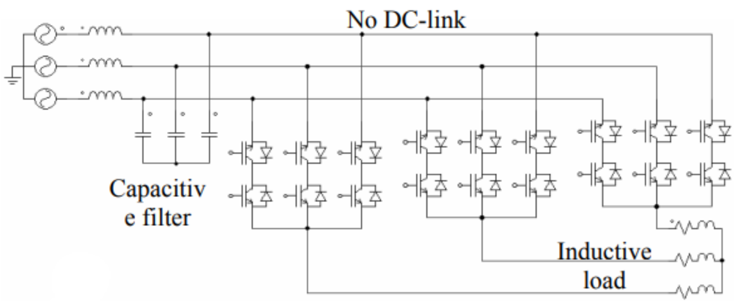


Figure 2.9: Matrix converter [15].

The advantages of using a matrix converter are the adjustable power factor, the high sinusoidal quality of the input and output waves and not using the bulky energy storage component [16].

However, matrix converters come with certain drawbacks. The large number of semiconductors and the absence of energy storage can lead to potential issues such as unbalanced supply voltages, voltage sags, and dips [16].

### 2.6.3 Hybrid Matrix converter

A hybrid matrix converter comprises two converters: a primary converter, primarily responsible for energy conversion, and an auxiliary converter tasked with addressing limitations inherent in the primary converter. These limitations typically include constraints on the power ratio between input and output and susceptibility to energy disturbances in the power supply [15].

## 2.7 Energy storage

The storage of energy produced by the generator, which can then be injected into the grid later or to supply loads when there is a shortfall in production can be realized using conventional batteries such as Lead-acid and Li-on, but Flow batteries can also be used.

Conventional batteries use oxidation-reduction reactions to produce energy. In these batteries, there is an anode responsible for supplying electrons, which is oxidized during the reaction, a cathode responsible for receiving electrons, which is reduced during the reaction, and an electrolyte that provides the medium for the transfer of energy. In the case of a Li-on battery, the anode is graphite and the cathode can be lithium cobalt oxide.

A comparison between various conventional batteries is presented in the table below.

Table 2.5: Comparison of conventional battery types [17]

| Type of batteries | Lead- acid | Ni-Cd | Li-ion | NaS |
|---|---|---|---|---|
| Energy Density (Wh/kg ) | 30-50 | 50-75 | 75-200 | 150-240 |
| Power Density (W/kg) | 75-300 | 150-300 | 150-315 | 150-230 |
| Cycle Life | 500-1000 | 2000-2500 | 1000-10000 | 2500 |
| Cost ($/kWh) | 150-200 | 400 | 600-800 | |

Flow batteries consist of two electrolyte solutions in different tanks, separated by a membrane. During charging and discharging, the flow of the electrolyte solution is achieved using pumps. In charging, oxidation of the electrochemically active material occurs at the anode and reduction of the electrochemically active material at the cathode. When discharging, the chemical reactions are reversed.

When integrating an energy storage system with a hydro energy production system, it enables the central facility to operate off-grid. However, in such scenarios, meticulous control of voltage, power, and load management becomes imperative. This stringent control is essential to regulate the system's loads and available energy production. In instances where the available energy falls short of meeting the demand, implementing load shedding becomes necessary to ensure sustained functionality of critical loads.

To use batteries in a micro-hydro system, we need electronic converters to connect to the grid and there are two possible options for making this connection:

- Connecting directly to the grid via a bidirectional AC-DC converter, topology A, as illustrated in Figure 2.10;

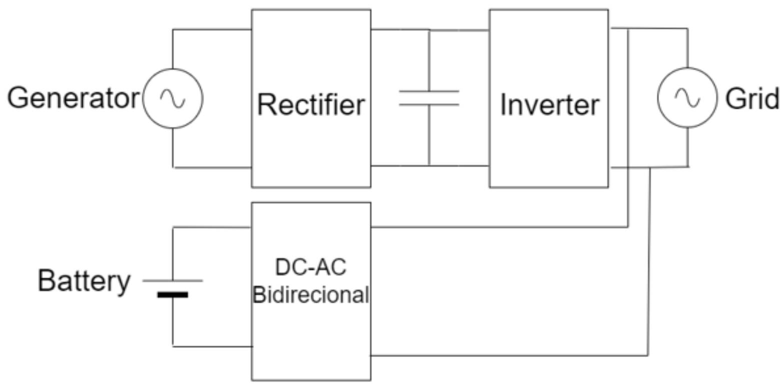


Figure 2.10: Topology A.

- Connecting to the DC bus in situations where the energy conversion from the generator to the grid is carried out with an AC AC converter with DC link, topology B, as indicated by Figure 2.11.

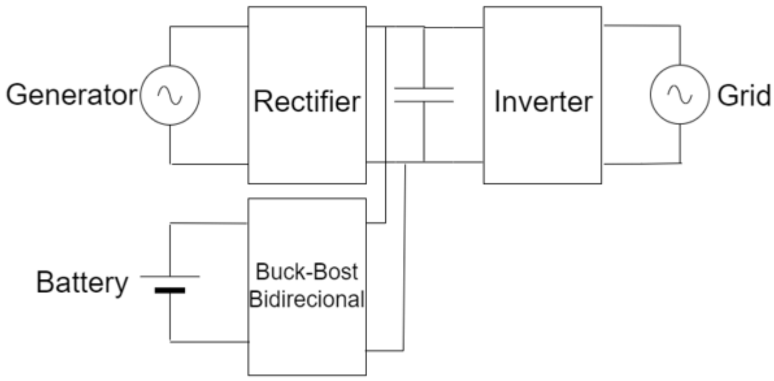


Figure 2.11: Topology B.

## 2.8 Products available on the market

Cost analysis is a crucial component of any project, especially when considering the implementation of micro hydropower stations. Research was carried out to determine the average prices of these systems in the current market.

Obtaining information on low-power hydraulic turbines proved to be a challenge, as the products available generally include both the turbine and the generator, and the products found in these situations were the following:

- 1 kW mini-hydro for drops of 5-30 meters and flows rates of 0.007 to 0.25 $m^3/s$ for about 180.74 €[18];

- 3kW hydro generator with a Kaplan turbine, for flow rates of $0.1m^3/s$ and drops of 2 to 6 meters for about 1100€ [19];

- 3kW hydro generator with a Pelton turbine, for flow rates of $0.03m^3/s$ and drops of 10 to 30 meters for about 1200€ [20].

For producing electricity, several motors have been identified that are suitable for this purpose. The motors chosen preferably had a high number of poles to have a lower rotational speed and an operating speed of S1 since the generation is expected to be continuous. Here are some examples:

- 2.2 kW three-phase induction motor with 8 poles and S1 speed, 476€ [21];

- 4 kW three-phase induction motor with 6 poles and S1 speed, 478€ [22].

Lithium batteries, which are among the most prevalent on the market, can significantly inflate the overall cost of a power station. The examples below are provided for a power station with a capacity of approximately 10 kW. However, these calculations can be adjusted to accommodate any power value.

- 3X PYLONTECH 48V lithium battery with a capacity of 3.6 kWh, 4421€ [23];
- 2X HUAWEI 360V LUNA2000 Lithium Battery Module 5 kWh, 6500€ [24];
- Tesla Powerwall, lithium batteries with a capacity of 13.5 kWh, approximately 8000€ [25].

The costs mentioned above are only for the battery modules, which would also require a BMS (battery management system) in certain cases.

To convert alternating current into direct current, a rectifier is crucial. Various types of rectifiers commonly used include:

- PF1000A-360, power module, 1.008 kW, 223.3€ [26];
- AOPs 1500, power module, 1.5 kW, 550.80€ [27].

## 2.9 Simulation and sizing software

One of the important parts of any project is the simulation, it's a crucial moment to check the viability of a project. To carry out a simulation, it can be use the following softwares:

- With the digital calculator from the Institute for Research and Technology it is possible to obtain the dimensions of the constituent elements of a Francis, Kaplan, or Pelton turbine. In the figures below it is possible to see an example of the sizing of a Francis turbine [28];

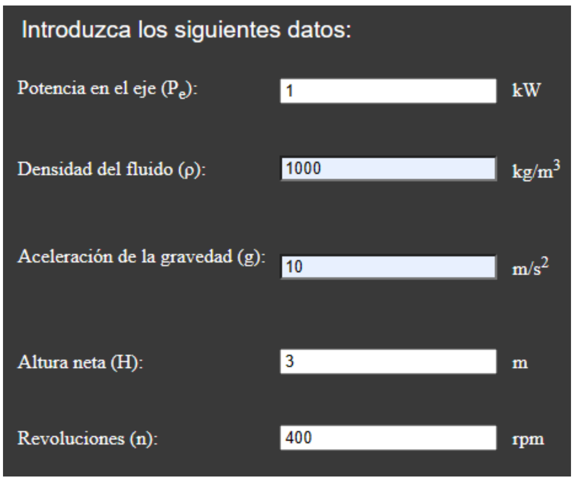


Figure 2.12: Sizing parameters[28].

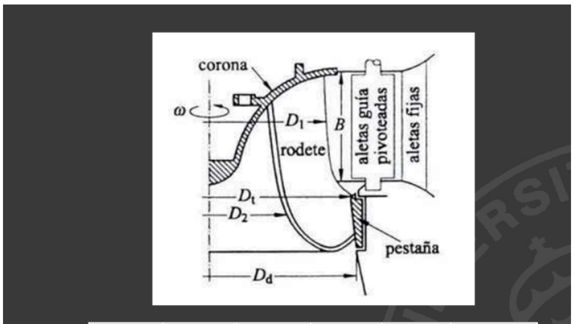


| $D_1$ [mm] | $D_2$ [mm] | $D_d$ [mm] | $D_t$ [mm] | [mm] | z [álabes] |
|---|---|---|---|---|---|
| 265 | 135 | 214 | 220 | 38 | 17 |

Figure 2.13: Sizing results[28].

- The software from Borst Engineering & Construction LLC is similar to the one above, but this one only allows the sizing of a cross-flow turbine [29] ;
- MATLAB is an excellent choice for simulating hydraulic turbines and electronic converters due to its extensive library of pre-built blocks and the ability to create customized components if needed;
- In addition to Matlab, Psim is also a suitable tool for testing converters. There are ready-made models for this or it can be built using individual components.

### 2.9.1 Simulation using Matlab Simulink

The utilization of MATLAB in this project stems from its unparalleled capability to simulate all pivotal elements outlined in this dissertation. The software's extensive array of resources for learning, coupled with its student licensing availability, makes it the optimal choice. Its multifaceted nature accommodates the simulation of critical components and serves as an invaluable tool for fostering comprehensive understanding and exploration within this study.

To simulate the conversion between the different DC voltages in the batteries and the DC bus, the "Bidirectional DC-DC Converter" block can be employed. This block, visible in Figure 2.14, is responsible for connecting the batteries to the DC bus.

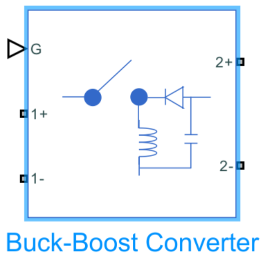


Figure 2.14: Bidirectional DC-DC Converter.

To connect the DC bus to both the grid and the batteries, the "Converter (Three-Phase)" block can be used. This block, which can be observed in the figure below, has bidirectional capability, allowing it to function as either a rectifier or an inverter.

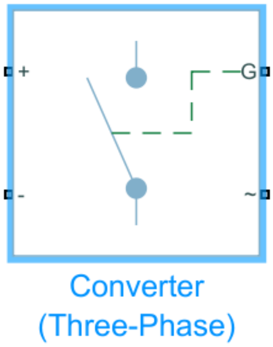


Figure 2.15: Three-phase converter.

The "Induction Machine Squirrel Cage" block can be employed to model a generator. This machine can be an induction generator, converting mechanical energy into electricity. Additionally, it includes a measurement port where it is possible to observe the rotor speed, power, voltages, and currents. The generator can be seen in Figure 2.16.

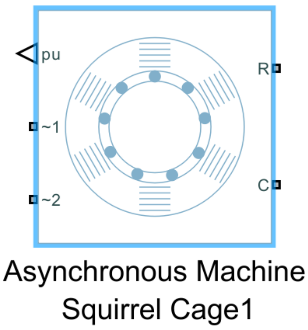


Figure 2.16: Induction motor.

# Chapter 3

# Bibliography review

In this dissertation, two projects with similar objectives were analyzed to enhance and refine the study. Each project presents its own set of advantages and disadvantages, contributing unique perspectives to the research.The projects are the following:

- Project A is "Dimensioning a Small Hydroelectric through the Utilisation and Transformation of Mills" carried out by engineer David Pereira Nogueira Gomez at the Faculty of Engineering of the University of Porto;
- Project B is "Design and Simulation of a Hybrid Microgeneration System Powered by Hydropower and Solar Photovoltaics" made by engineer Valdecir Junior De Paris at the at the Federal University of Santa Catarina.

## 3.1 Project A

In this project, the objective was to convert a mill by the Sousa River into a mini hydroelectric power station. Throughout this endeavor, a comprehensive technical and economic analysis was conducted. This transformation aimed to harness the river's energy potential and contribute to sustainable power generation in the region.

In the pursuit of gathering data on the river flow near the mill, encountering significant limitations arose. Specifically, the available information solely pertained to a hydrometric station located several kilometers away. Moreover, within this distance, additional tributaries had already merged into the main river, rendering the data from this station inadequate and irrelevant to the immediate vicinity of the mill.

Consequently, an alternative approach was undertaken. Data from a river with comparable characteristics was utilized as a substitute. The following table showcases the data according to the flow of the water.

Table 3.1: Flow of the river in function of the number of days [6]

| Flow ($m^3/s$) | Number of days | % of the year |
|---|---|---|
| >20 | 3 | 0.7 |
| >15 | 6 | 1.5 |
| >10 | 15 | 4.0 |
| >9 | 19 | 5.1 |
| >8 | 24 | 6.6 |
| >7 | 33 | 9.1 |
| >6 | 47 | 12.8 |
| >5 | 70 | 19.1 |
| >4.5 | 83 | 22.6 |
| >4 | 109 | 29.7 |
| >3.5 | 136 | 37.2 |
| >3 | 159 | 43.5 |
| >2.5 | 188 | 51.4 |
| >2 | 210 | 57.2 |
| >1.5 | 233 | 63.7 |
| >1 | 272 | 74.3 |
| >0.4 | 318 | 86.9 |
| >0.02 | 365 | 100 |

Given the data outlined above and considering the limited head height available at the site, engineer David Nogueira opted for the implementation of Kaplan turbines. This decision was primarily driven by their adaptability across a broader range of flow rates and their superior efficiency, particularly in situations with lower flow rates.

After the selection of the turbine, the assessment focused on the operation of the power station with a single generator group, yielding the following values for energy production and costs, and they are described in Table 3.2.

Table 3.2: Comparison between the two typologies for the central

| | Case with 1 group | Case with 2 group |
|---|---|---|
| Cost of implementation (k€) | 201 | 242 |
| Annual production (MWh) | 603 | 632 |
| Investment payback (years) | 8.7 | 10.7 |

The introduction of a second generator enhances the energy output. However, it requires a higher initial investment, and the payback period for this investment is also longer. This comparison between the two typologies for the central highlights a trade-off between increased energy production and the higher initial and long-term costs associated with the additional group.

## 3.2 Project B

In this project, the primary aim is to simulate an integrated system that combines both hydroelectric and solar energy sources, capitalizing on their mutual complementarity. The objective is establishing a comprehensive model that showcases the synergy and mutual support between these renewable energy forms.

In contrast to the previous project and the proposed simulation in this dissertation, a water reservoir exists within this project framework. This reservoir serves as a pivotal component, fundamentally altering the dynamics of energy generation and storage. Its presence enables the strategic accumulation of water, allowing for more nuanced control over the hydroelectric energy generation process.

The project's topology is depicted in the figure below.

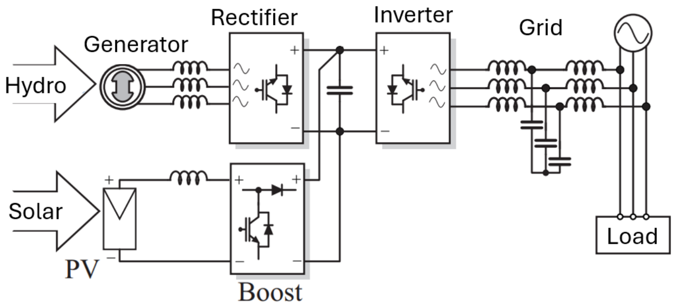


Figure 3.1: Proposed topology [10].

As this system has a reservoir at times of solar production, it is possible to use this energy to support the system and thus reduce water production at these times and store water for future use. As a result, dependence on the grid is greatly reduced, as can be seen in Figure 3.2.

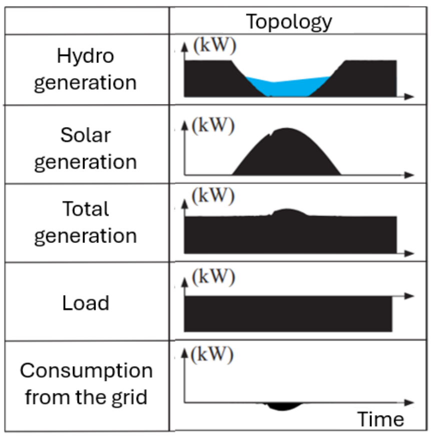


Figure 3.2: Variation in production and consumption over time [10].

Despite its comprehensive features and ability to function off-grid effectively, the project's intricate nature and substantial financial investment may present challenges.

## 3.3 Project A vs Project B

The comparison between Project A and Project B delineates distinct attributes in their design and functionality. Project A, while simpler and easier to implement, is particularly geared towards low-drop scenarios, exhibiting readiness for such situations. Conversely, Project B represents a more intricate endeavour. Its integration with solar power enables energy generation even during periods of low river water flow. However, it's worth noting that Project B was specifically designed for a moderate waterfall.

## 3.4 Contributions of Projects A and B

### 3.4.1 Project A

Project A contributes significantly to this initiative by providing comprehensive insights into the process of designing a low-head mini-hydropower project and outlining the essential steps for its implementation.

The project also delves into the necessary legal frameworks, examining key legislative decrees that warrant attention. This includes an in-depth economic analysis that elucidates the critical indicators and offers a comprehensive overview of the implementation costs associated with a mini-hydropower plant.

Moreover, the project exemplifies the meticulous process of designing the feeder canal, highlighting primary considerations, especially regarding its capacity to deliver an adequate flow for the intended power output. This involves a detailed exploration of sizing considerations and potential challenges in ensuring the channel's efficiency.

Furthermore, the project provides a detailed illustration of the turbine sizing process, focusing on the Kaplan turbine. This encompasses a thorough analysis of the turbine's dimensions, operational characteristics, and performance parameters.

In essence, Project A not only offers valuable insights into the intricacies of low-head mini-hydropower project design but also addresses legal aspects, conducts a thorough economic analysis, and illustrates the dimensioning processes for both the feeder canal and the chosen turbine.

### 3.4.2 Project B

Project B significantly enhances this dissertation by offering a distinct perspective on the integration of an alternative energy source, specifically solar energy, drawing parallels to the incorporation of batteries. This unique viewpoint contributes to a more comprehensive understanding of diversified energy integration within the scope of this study.

The contribution is evident in its exploration of the impact of integrating photovoltaic energy into the hydroelectric plant, shedding light on the consequential effects on electricity production. By providing a detailed analysis of both turbine and rotor sizing within the pipeline, as well as the injector nozzle, Project B adds a layer of intricacy to the examination of these vital components.

Furthermore, the meticulous examination of converter sizing and control adds depth to the overall analysis. Project B goes beyond the surface by delving into the nuanced aspects of converter sizing and elucidating the intricacies of control mechanisms.

The inclusion of simulations using tools such as PSIM and real-time simulations with Typhoon HIL software is another noteworthy contribution. This not only showcases the practical application of the proposed components but also provides a tangible demonstration of their performance in various scenarios.

# Chapter 4

# Proposed system

For the hydroelectric generating system, an ideal scenario involves powering a small store equipped with a refrigerator, a freezer, and lighting. The system is primed for efficient hydroelectric power generation, situated near a river boasting falls of at least 2 meters and consistently high flow rates, typically exceeding $0.23m^3/s$. This setup capitalizes on the natural resource of flowing water to drive turbines and generate electricity, providing a sustainable energy solution for the store's operations. With reliable access to renewable energy, the store can operate independently of the grid, ensuring uninterrupted power supply for essential appliances and lighting needs.

The values of 2 meters for the fall and 0.23 $m^3/s$ for the flow rate were chosen because they are commonly met in Portuguese rivers. These criteria ensure that the hydroelectric generating system can be effectively implemented in many locations across Portugal, leveraging the country's natural water resources to provide consistent and sustainable energy.

## 4.1 Loads

In the table below, the loads and the quantity of each equipment are presented. It was determined that the number 30 represents a plausible value for the situation where the store incorporates a small pathway.

Table 4.1: Loads

| Equipment | Quantity | Power (W) | Total Power (W) |
|---|---|---|---|
| Light Post | 30 | 60 | 1800 |
| Freezer | 1 | 38 | 38 |
| Refrigerator | 1 | 28 | 23 |

The power consumption of various loads fluctuates according to the time of day. While certain loads, such as the freezer and fridge, remain constant, lighting varies across four levels. These levels include all lights turned on, 50% of lights turned on, 25% of lights turned on, and all lights turned off. These variations in power levels are detailed in Table 4.2.

Table 4.2: Power levels according to the loads

| Power Level | Loads | Total power (W) |
|---|---|---|
| 1 | All loads | 1861 |
| 2 | Freezer, fridge and 50% of lights | 961 |
| 3 | Freezer, fridge and 25% of lights | 511 |
| 4 | Freezer, fridge | 61 |

According to previous table it was possible to come up a graphical representation of the variance of the load during the day, represented by Figure 4.1. It's noticeable that the loads are higher during the night compared to daytime, as expected, due to substantially lower luminosity. Conversely, during the day, power consumption mainly revolves around the freezer and fridge, as ample natural light reduces the need for artificial lighting.

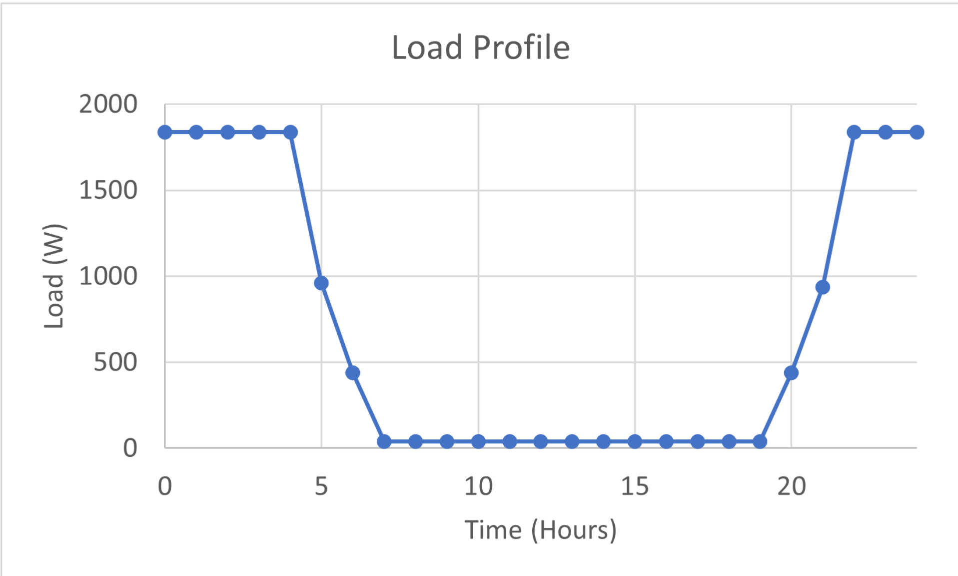


Figure 4.1: Load Profile

## 4.2 Battery

This application's capacity of 10,000 Wh was deemed sufficient to accommodate typical power demands. In cases of low production, loads can be substantially reduced to prioritize refrigeration. Even with the battery's small state of charge and no energy being produced by the generator, the system can sustain operations for an extended duration, as demonstrated in Table 4.3.

Table 4.3: Autonomy of Loads at Different SOC

| SOC | Loads | Time Remaining (h) |
|---|---|---|
| 100% | Autonomy for all loads | 5.37 |
| | Autonomy for freezer, fridge, and 50% of lights | 10.41 |
| | Autonomy for freezer, fridge, and 25% of lights | 19.57 |
| | Autonomy for freezer and fridge | 163.93 |
| 75% | Autonomy for all loads | 4.03 |
| | Autonomy for freezer, fridge, and 50% of lights | 7.80 |
| | Autonomy for freezer, fridge, and 25% of lights | 14.68 |
| | Autonomy for freezer and fridge | 122.95 |
| 50% | Autonomy for all loads | 2.69 |
| | Autonomy for freezer, fridge, and 50% of lights | 5.20 |
| | Autonomy for freezer, fridge, and 25% of lights | 9.78 |
| | Autonomy for freezer and fridge | 81.97 |
| 25% | Autonomy for all loads | 1.34 |
| | Autonomy for freezer, fridge, and 50% of lights | 2.60 |
| | Autonomy for freezer, fridge, and 25% of lights | 4.89 |
| | Autonomy for freezer and fridge | 40.98 |

## 4.3 Control

### 4.3.1 Grid Connected with low power flow to the grid

The following strategy was proposed in the context of grid-connected operations, emphasizing minimizing traffic between the grid and the hydropower station. By minimizing interactions with the grid, there is a more extensive use of the batteries, which can promote a reduction in energy expenses, especially in high electricity prices. Utilizing stored energy can be more cost-effective during these periods.

Moreover, optimizing the utilization of battery storage and hydropower production can achieve this goal for a store aiming to maximize the use of green energy. This approach ensures that the energy consumed is predominantly renewable, aligning with sustainability objectives.

Additionally, relying on stored power can provide better quality electricity, as it mitigates issues related to grid fluctuations and interruptions.

The following strategy was proposed below.

Primarily, when power generation exceeds 99% of the capacity, the generator serves the load demand while channeling surplus energy into the grid. When production is low, the batteries step in to provide the required power to meet the load demands.

Furthermore, during periods of elevated power production and ranging between 25% and 99% capacity, the generator fulfills load requirements while directing excess power toward battery storage. This dual-purpose utilization ensures efficient energy storage for later use, enhancing system flexibility and resilience. In cases where production is low, the batteries compensate by supplying the necessary power to meet the load requirements.

In scenarios where power generation falls below 25% capacity, a multi-faceted approach is adopted to maintain operational continuity. Here, the generator prioritizes battery charging to increase storage reserves, while the grid supplements power deficits and also contributes to battery charging. Simultaneously, load demands are met predominantly by grid-supplied electricity, ensuring uninterrupted service even during periods of lower power generation.

### 4.3.2 Grid Disconnected

In scenarios where the grid becomes disconnected, the management of power generation is essential.

Firstly, when the charge level exceeds 99%, the generator is tasked solely with supplying the load. In insufficient power, batteries serve as a complementary source, ensuring continuous operation.

Secondly, when the charge level falls between 30% and 99%, power generated caters to the load and facilitates battery charging during surplus. Conversely, batteries seamlessly supplement the loads during power deficits to maintain operational stability.

Thirdly, load-shedding measures are implemented to expedite the charging process if the battery charge dips below 30% but remains above 15%. This strategic reduction in non-essential loads optimizes resource allocation for faster battery replenishment.

Lastly, in critical situations where the battery charge plummets below 15%, only essential loads remain connected, safeguarding vital operations until the grid is restored or additional power sources become available.

### 4.3.3 Grid Connected and battery as backup storage

In scenarios where batteries primarily serve as backup storage, an optimized operational framework ensures their readiness while minimizing grid reliance.

Under normal conditions, the generator and grid are tasked with charging the batteries, with the generator granted priority to ensure consistent battery replenishment. This concerted effort aims to maintain optimal battery charge levels, reinforcing backup capacity for unforeseen grid disruptions. Concurrently, the grid predominantly meets load demands, leveraging its reliability and accessibility. This strategic allocation of resources ensures efficient utilization of grid-supplied power while preserving battery reserves for emergency scenarios.

In the event of grid failure, operations seamlessly transition to the contingency plan explained above, where the generator assumes a central role in charging batteries and supplying the loads, guaranteeing uninterrupted service until grid restoration or alternative power sources become available.

## 4.4 Simulations

This section presents simulations conducted in Simulink, serving as tests for the developed system. These simulations employ simplified models for each component, with a gain factor representing each one. This simplification was necessary due to the challenges of simulating all components together in a more complex manner. However, each block will be elucidated further in the dissertation. Figure 4.2 illustrates the components represented, while the circuits and programs used in MATLAB are detailed in the annexes.

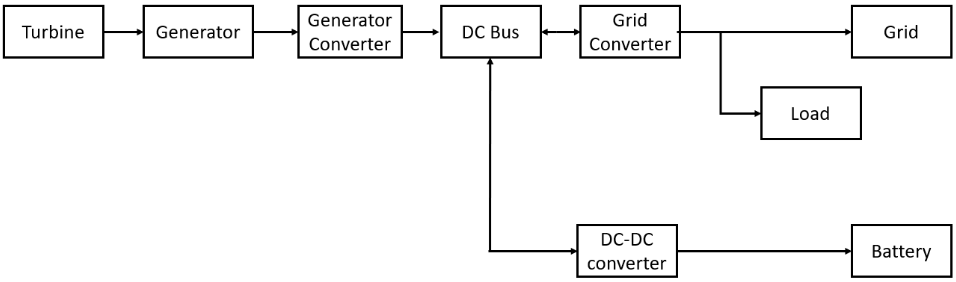


Figure 4.2: Circuit.

The turbine's efficiency is estimated to be approximately 88%, while the generator exhibits an efficiency of 87%. Additionally, the converters demonstrate an efficiency of 95%. These parameters form the foundation for the system's initial performance considerations.

### 4.4.1 Grid Connected with low power flow to the grid

The following simulation assumed that the grid is connected and that river exhibits a substantial flow, consistently enabling maximum power generation and that the grid is connected. Consequently, the available power at the output of the generator converter is determined by the product of the maximum power rating of the turbine and the efficiencies of the turbine, generator, and converter. This can be represented mathematically as shown in the equation below:

$$P_{converter} = 4000 \times 0.88 \times 0.86 \times 0.95 = 2876W \tag{4.1}$$

Figure 4.3 depicts the variations of power levels according to the time of day. It's noticeable that the loads are higher during the night compared to daytime, as expected, due to substantially lower luminosity. Conversely, during the day, power consumption mainly revolves around the freezer and fridge, as ample natural light reduces the need for artificial lighting.

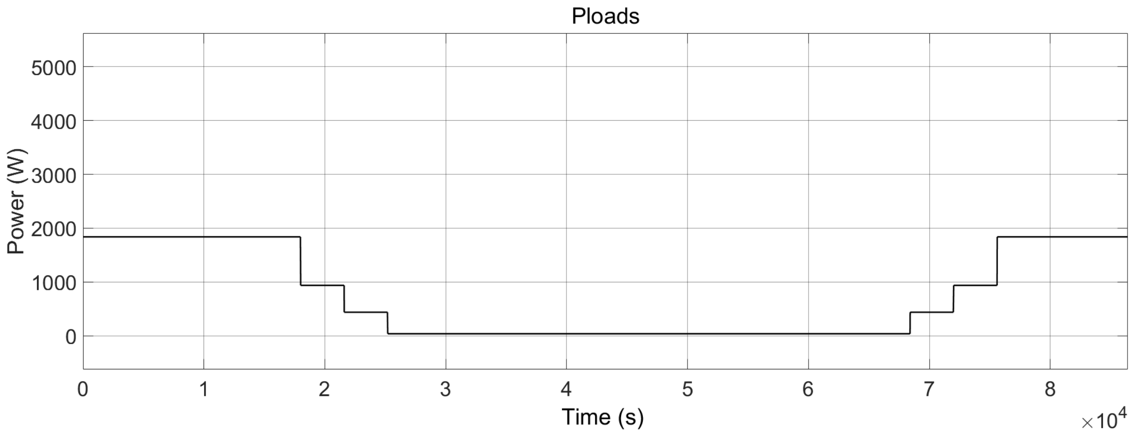


Figure 4.3: Variation of loads during 24 hours.

As depicted in Figure 4.4, the initial SOC is at 5%. Consequently, the system's primary objective is to expedite the charging process, requiring the charging power to operate at full capacity. As illustrated in Figure 4.5, all the power produced is directed towards the battery, with additional power drawn from the grid to assist in the charging process. As a result, the power injected into the grid assumes a negative value. Upon reaching a SOC of 25%, it becomes apparent that the charging rate begins to taper off. This phenomenon is attributable to the generator responsible for supplying power to the loads, with the surplus allocated towards charging. Upon completion of the charging cycle, the generator redirects all surplus power to both the grid and the loads.

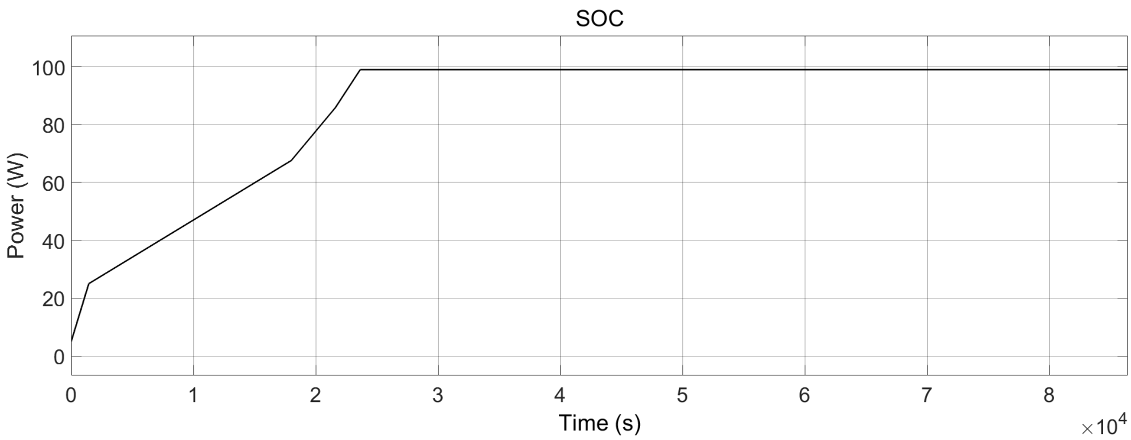


Figure 4.4: State of charge of the battery.

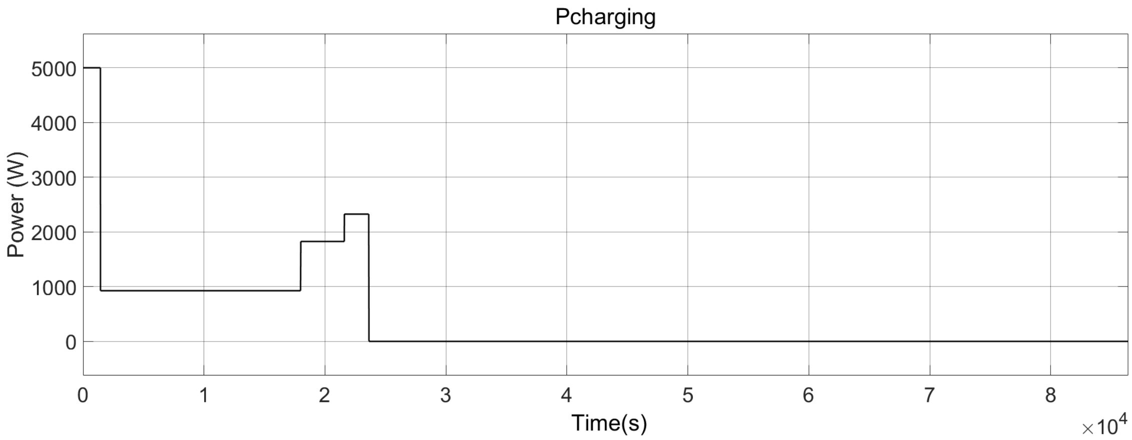


Figure 4.5: Charging power of the battery.

Upon analyzing Figures 4.6 and 4.7, it becomes visible that the power injected into the grid consistently equals the power before the loads minus the power consumed by the loads.

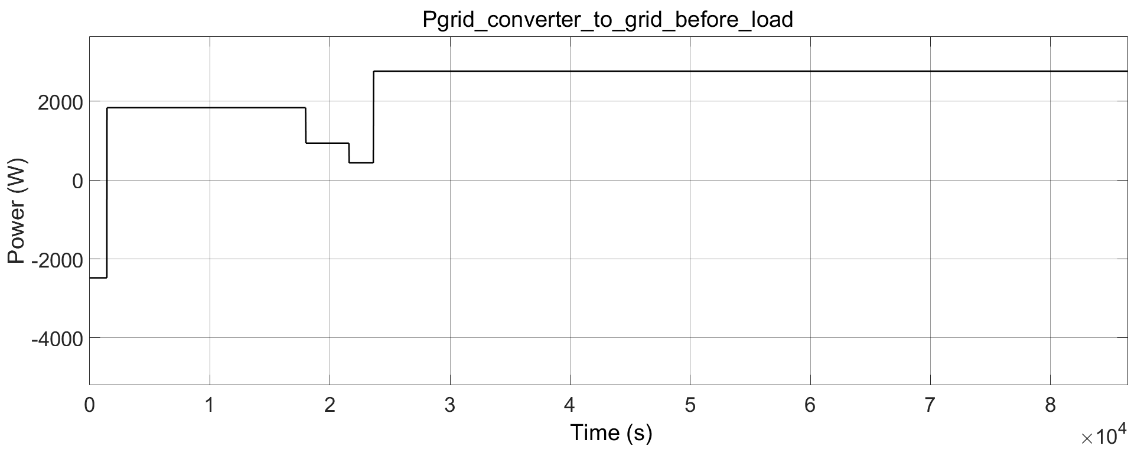


Figure 4.6: Power in direction to the grid before the load.

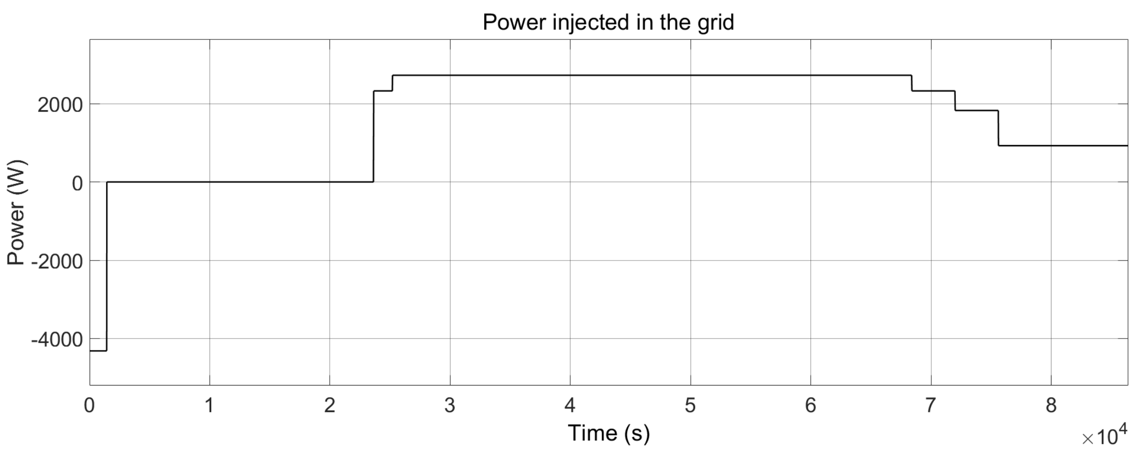


Figure 4.7: Power injected in the grid.

### 4.4.2 Grid Disconnected

In this simulation, the initial SOC remains consistent with the one employed previously, leading to load shedding within the load, as evidenced in Figure 4.8. Initially, the load is minimal, increasing its power demand gradually as the SOC reaches 15%. Upon reaching a SOC of 30%, the load profile resembles that observed previously, indicating an absence of load shedding.

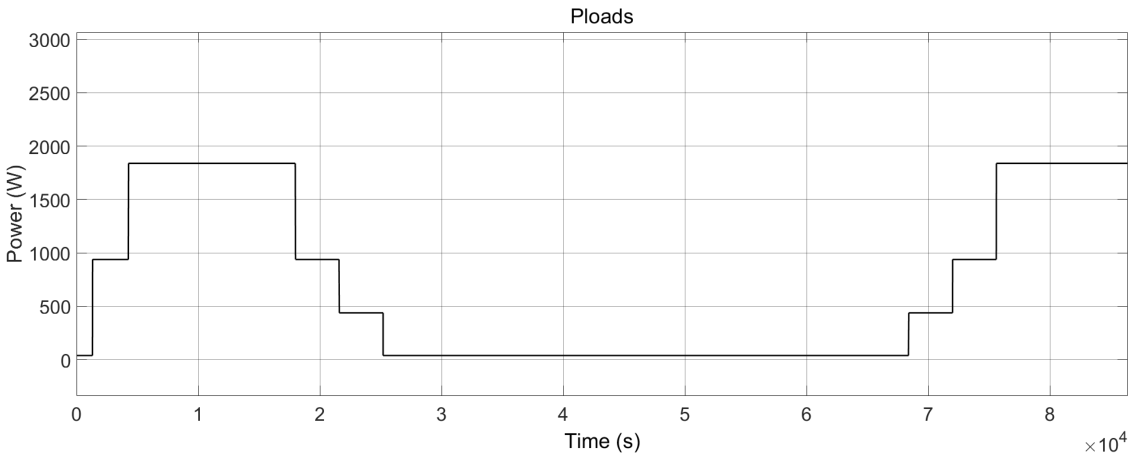


Figure 4.8: Variation of loads during 24 hours.

The charging rate in this simulation experiences a notable deceleration due to the reliance solely on the generator for charging, as depicted in Figures 4.9 and 4.10.

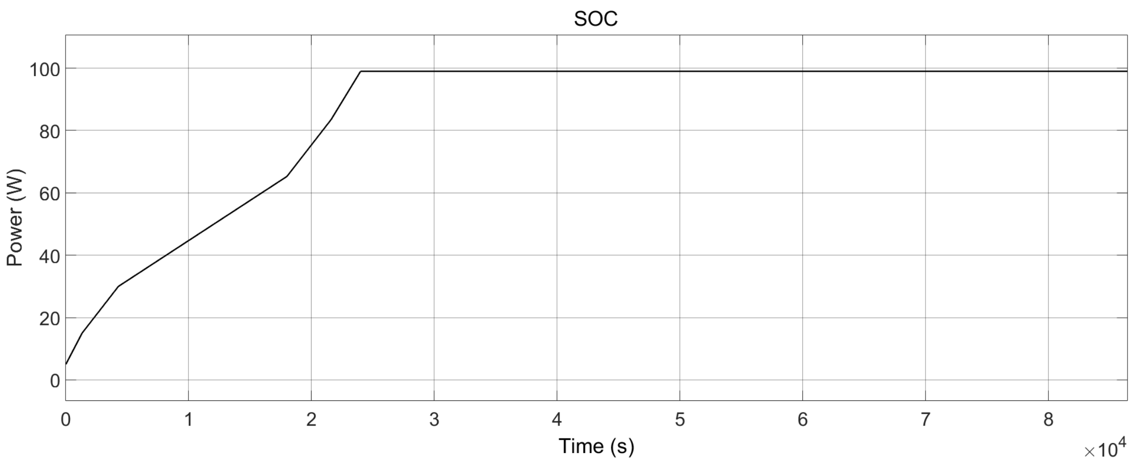


Figure 4.9: State of charge of the battery.

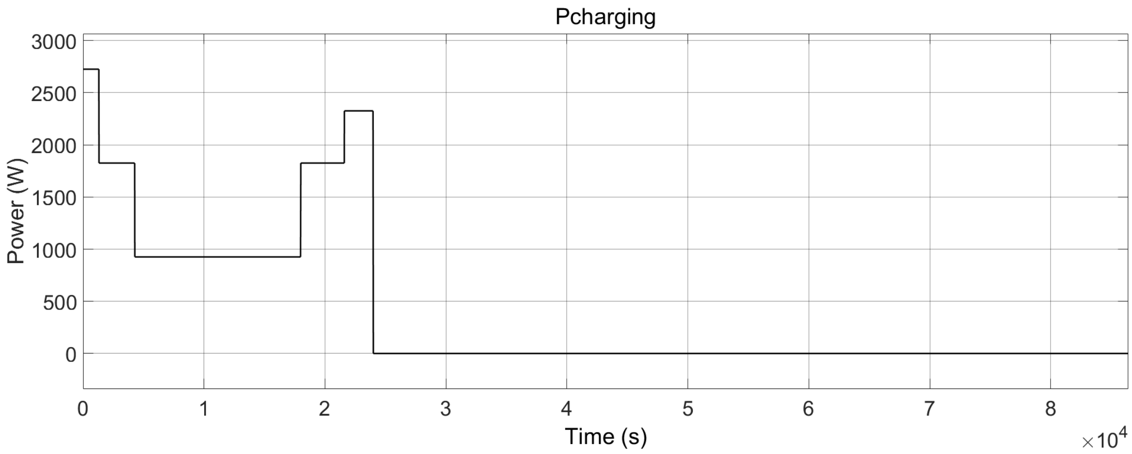


Figure 4.10: Charging power of the battery.

As anticipated, there is no power exchange between the grid and the system since they remain disconnected, as illustrated in Figure 4.11. Moreover, the transferred power is adequate to meet the demands of the loads, as depicted in Figure 4.12.

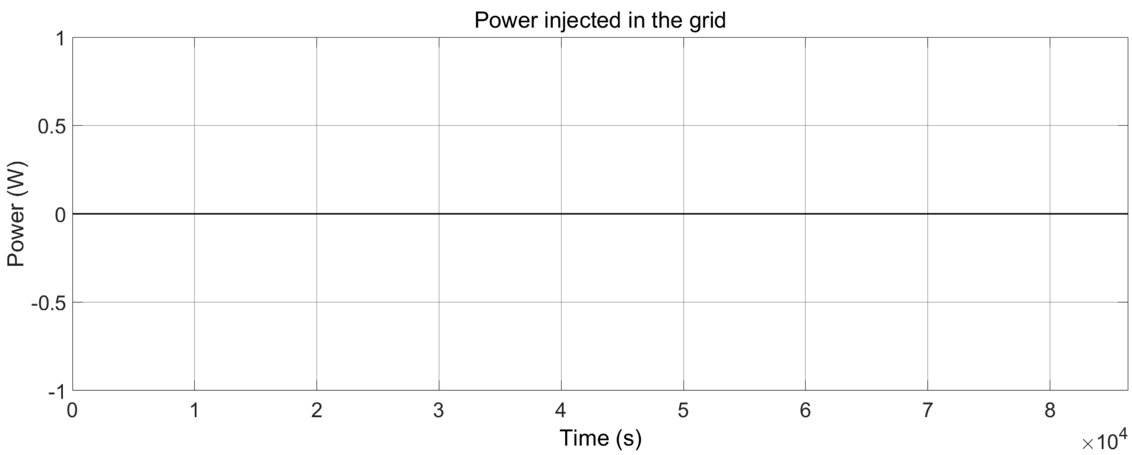


Figure 4.11: Power injected in the grid.

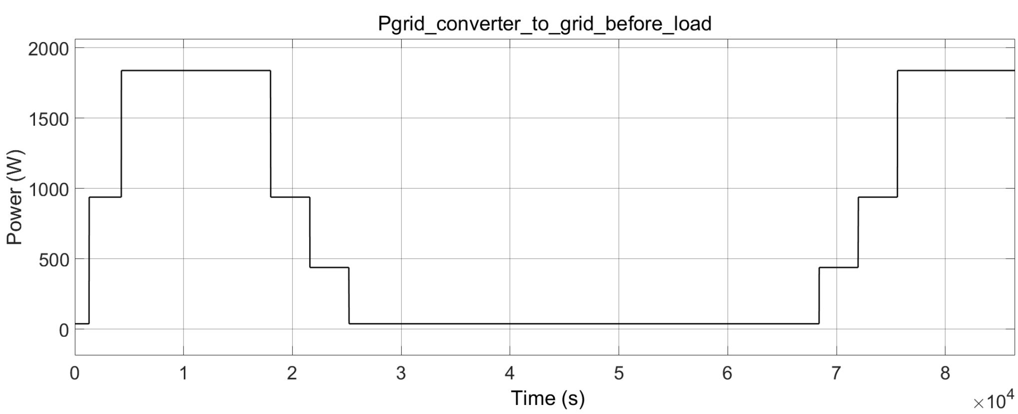


Figure 4.12: Power in direction to grid before the load.

### 4.4.3 Grid Connected and battery as backup storage

We maintain continuity with previous simulations in this iteration by retaining the identical load profile and initial SOC.

In this simulation, the battery functions primarily as a backup power source, prioritizing full charging when the grid is connected to remain on standby for times of need. This behavior is evident in Figure 4.13 and 4.14, where the SOC consistently increases without fluctuation, maintaining a continuous state of full charge until the battery reaches its capacity.

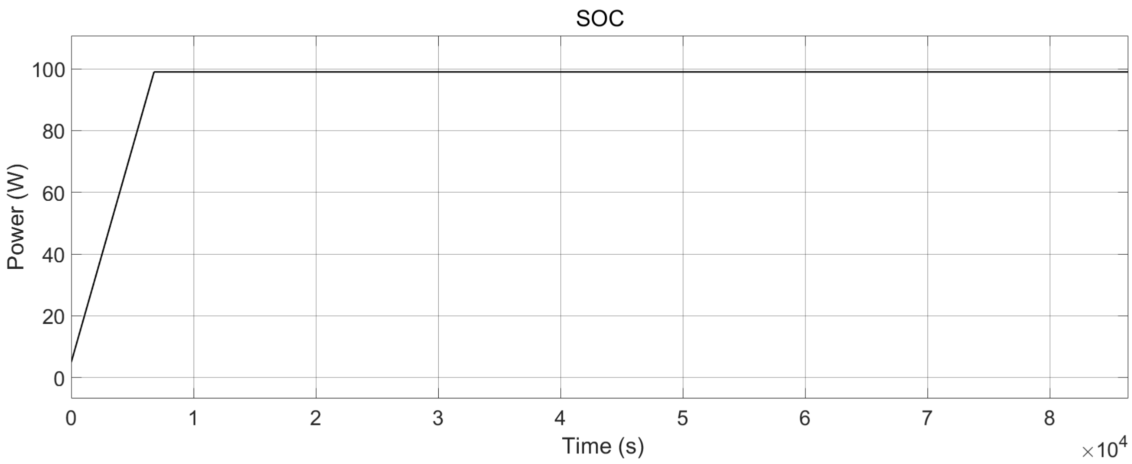


Figure 4.13: State of charge of the battery.

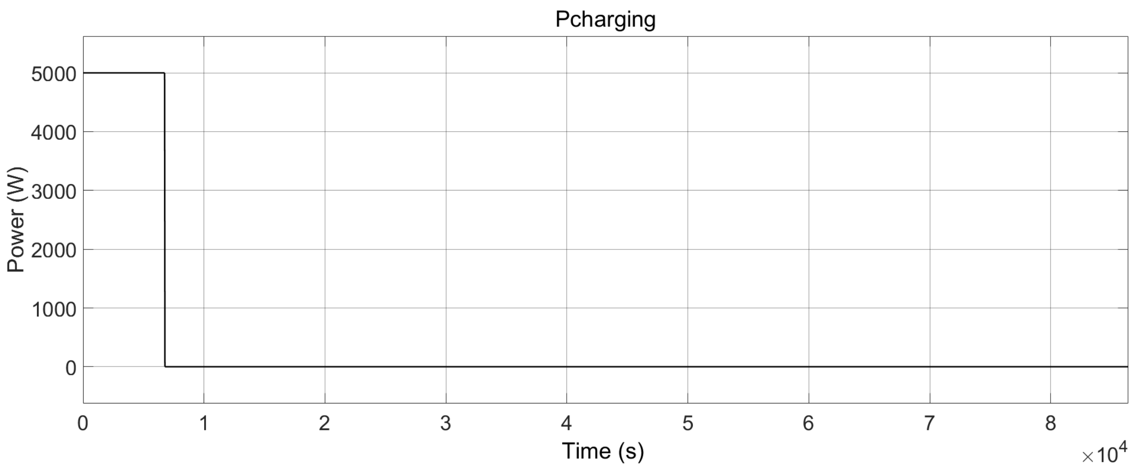


Figure 4.14: Charging power of the battery.

In Figure 4.15, a clear pattern emerges: once the battery reaches full charge, all available power is directed towards both the grid and the loads.

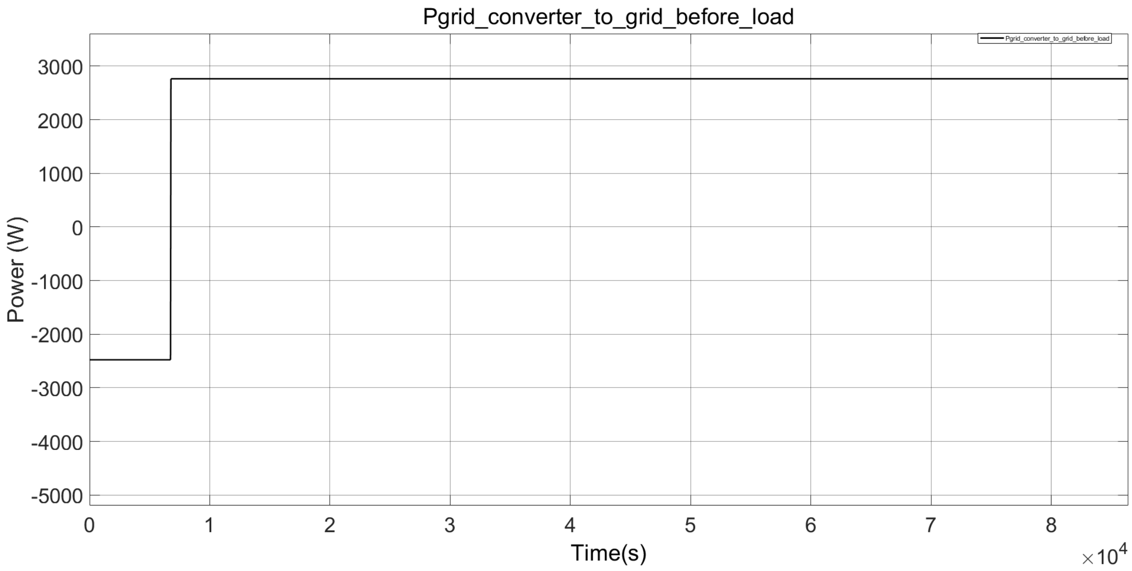


Figure 4.15: Power in direction to grid before the load.

### 4.4.4 Grid connected from t=0s to t=10.000s

A dynamic model was employed for this simulation. Initially, for the first 14.400 seconds, the river exhibits its full potential to supply power. However, after this period, its capacity diminishes to only being able to supply 1000W to the turbine. The battery system is configured solely as a backup plan and is activated when necessary. Additionally, the grid is initially connected but disconnects at the 10.000-second mark.

Examining the figure below, we can discern that before the 10.000-second mark, when the grid is still connected, it supplements the battery charging process by drawing power from the grid. Subsequently, once the battery reaches its full charge, all surplus power is sent to the grid. After the disconnection of the grid, the power flow shifts, with energy being solely distributed to meet the demands of the loads.

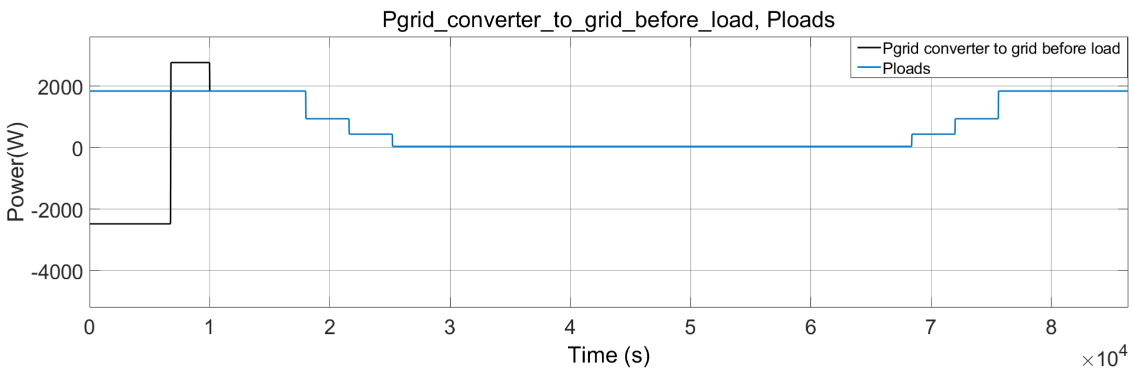


Figure 4.16: Variation of loads and power in direction to the loads and grid.

Upon analyzing Figures 4.17 and 4.18, discernible variations in the SOC become evident following the grid's disconnection and the reduced quantity of power generated. This outcome aligns with expectations, considering that the river experiences a reduced flow and only has a potential of 1000W, while the loads at the moment of variation are approximately 2000W. The SOC only recovers to full charge when the loads are reduced.

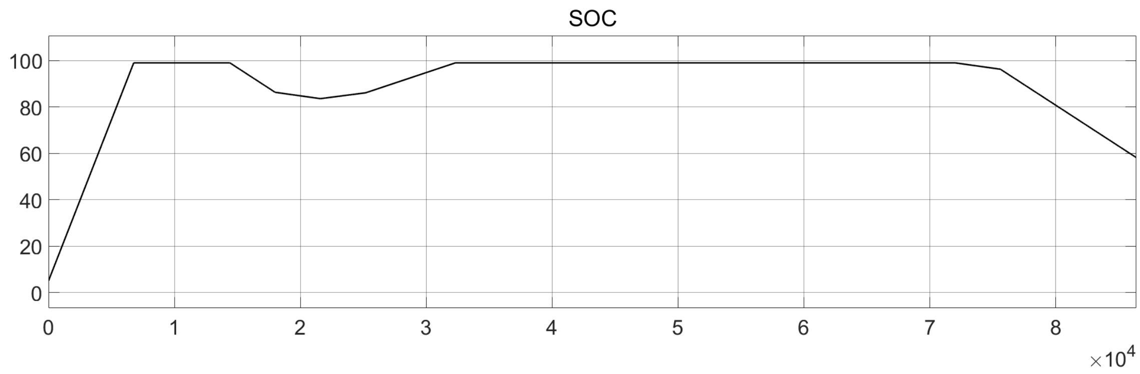


Figure 4.17: State of charge of the battery.

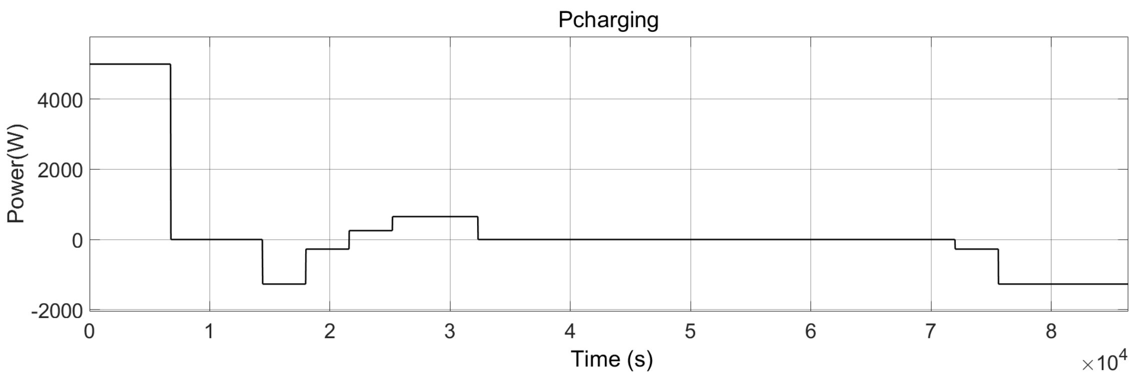


Figure 4.18: Charging power of the battery.

# Chapter 5

# Individual systems

## 5.1 Buck-Boost

The buck-boost converter, renowned for its capability to dynamically adjust downward and upward voltage levels, is a pivotal component in contemporary energy systems. Its versatile nature allows output voltage modulation, enabling input power conversion to levels conducive to various operational requirements. This adaptability arises from the converter's ability to function in multiple modes, facilitating either voltage reduction -buck mode- or amplification -boost mode-based on operational demands.

In contexts such as energy storage and renewable energy systems, where efficient power management is paramount, the buck-boost converter emerges as an indispensable tool. Its bidirectional current flow enables seamless integration into diverse applications, including the charging infrastructure of electric vehicles.

The converter employs two switches that can be controlled using a Pulse Width Modulation (PWM) signal. This signal utilizes a duty cycle as its input parameter.

### 5.1.1 Circuit

The diagram below shows the conventional circuit configuration employed in a buck-boost converter. This topology necessitates the utilization of essential components comprising two capacitors, one inductor, and two controlled switches. These components collectively orchestrate the intricate voltage regulation and conversion process inherent to the buck-boost operation. It is also important to mention that it is possible to analyze the complete scheme that gathers the control as well as the buck-boost in Appendix A.1.

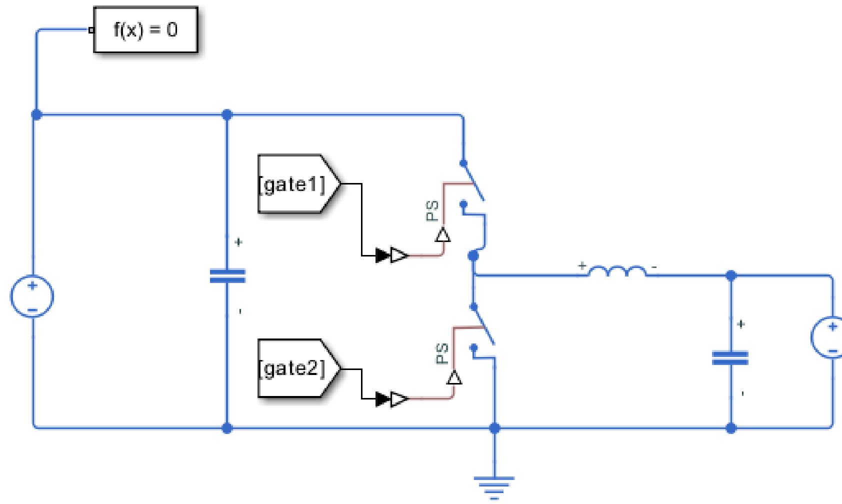


Figure 5.1: Buck-Boost converter.

### 5.1.2 Switching frequency

The switching frequency employed for the converter was set at 10 kHz, a frequency widely adopted within the realm of such converters. Notably, a higher frequency can improve losses in passive components due to reduced ripple currents and smaller component sizes. However, it is essential to acknowledge that higher frequencies can also escalate losses in the switching devices. Despite this trade-off, the selection of 10 kHz strikes a balance between minimizing passive component losses and managing switching device losses effectively.

### 5.1.3 Sizing components

The inductor and capacitor play crucial roles in the boost mode. The inductor stores energy as a magnetic field when current passes through it. During the switch's closure, it accumulates energy, and when open, it helps adjust the output voltage.

On the other hand, the capacitor smooths the output voltage. When the switch is closed, it charges; when open, it regulates the output voltage. These components work in tandem to convert input voltage to a higher output voltage, making the converter a vital component in various applications.

In a buck converter, the functions of the inductor and capacitor are similar but with some differences due to the different operating principles of the converters. The inductor releases energy to maintain the output voltage when the switch is closed and charges during closure. The capacitor serves a similar role in both converters.

In Table 5.1, the formulas for sizing the passive components required for the buck-boost converter are provided.

Table 5.1: Calculation formulas for inductor and capacitors in buck and boost converters [30][31]

| **Type of converter** | **Inductor** | **Capacitor** |
|---|---|---|
| **Buck** | $L = \frac{(V_{in}-V_{out})\times D}{f_s \times \Delta I_L}$ | $C = \frac{\Delta I_L}{8\times f_s \times \Delta V_{out}}$ |
| **Boost** | $L = \frac{V_{in}\times(V_{out}-V_{in})}{f_s \times \Delta I_L \times V_{out}}$ | $C = \frac{I_{out}\times D}{f_s \times \Delta V_{out}}$ |

In Table 5.2, the calculated values of the passive components required for the buck-boost converter are provided. Here, $C_1$ corresponds to the capacitor sized for the boost mode, $C_2$ corresponds to the capacitor sized for the buck mode, and L represents the largest value obtained from sizing in both buck and boost modes.

Table 5.2: Results of capacitor and inductance values for the converter

| L | $C_1$ | $C_2$ |
|---|---|---|
| 0.05376 | 1.09E-05 | 5.43e-7 |

### 5.1.4 Simulation

In the subsequent section, a simulation of the buck-boost converter was conducted utilizing the parameters outlined in Table 5.3.

Table 5.3: Parameters of Buck-Boost converter

| V1 (V) | V2 (V) | L (H) | C1 (F) | C2 (F) | Fs (kHz) |
|---|---|---|---|---|---|
| 800 | 240 | 0.05376 | 1.09E-05 | 5.43e-7 | 10 |

Current control was employed for this converter, as depicted in Figure 5.2. This control strategy begins by calculating from a power reference and then comparing the voltages to the current in the inductor. Subsequently, it utilizes a PI controller.

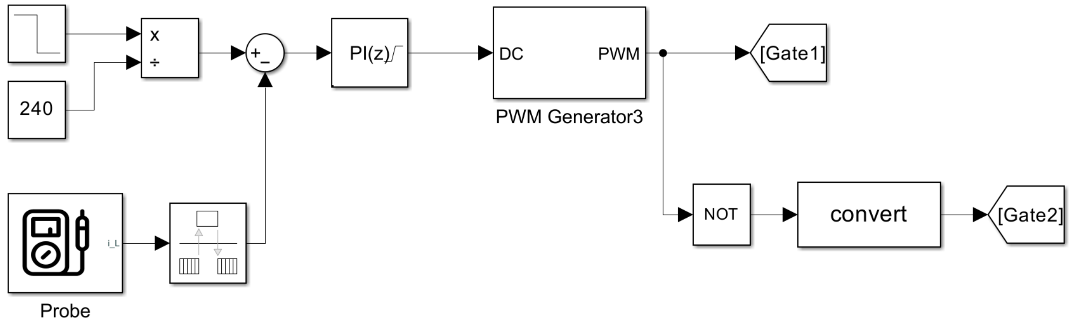


Figure 5.2: Buck-Boost converter control.

#### 5.1.4.1 Simulation V1=800 V, V2=240 V, P=4000 W and P=-2000 W of t=0.3 to 0.6s

Upon observing Figure 5.3, it becomes apparent that the converter is functioning as anticipated. The power value aligns with the reference, exhibiting only a slight disturbance due to the transient response from the change in the reference signal.

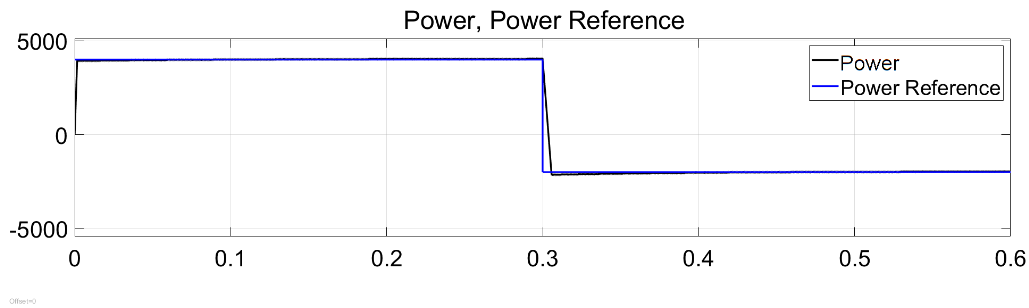


Figure 5.3: Buck-Boost converter simulation.

## 5.2 Grid Converter

A grid converter is an essential device that facilitates the connection of renewable energy sources, such as micro-hydropower systems, to the electrical grid. It acts as an intermediary, converting the electricity generated by the power system into a format that is compatible with the grid and suitable for use in residential and commercial settings. Without this conversion, the energy produced by renewable sources would not meet the necessary standards for grid compatibility, rendering it unusable for everyday electrical applications.

The six-switch converter is a cornerstone in contemporary power electronics, renowned for its efficiency and versatility in bidirectional power conversion between DC and AC. Its distinctive design enables precise control over voltage levels, rendering it a multifaceted tool capable of meeting diverse operational demands. This adaptability is underscored by its ability to seamlessly transition between various operating modes, including rectification and inversion, accommodating different power levels and types as required.

Due to its bidirectional power flow capability, the six-switch converter is pivotal in renewable energy integration and grid-tied systems. Its seamless integration into applications such as solar photovoltaic systems and grid-connected renewable energy sources underscores its significance in facilitating sustainable energy solutions. By efficiently utilizing renewable energy resources, the converter contributes significantly to advancing the transition towards a cleaner and more sustainable energy future.

In technical terms, the grid converter transforms the electrical output from the renewable energy system into an AC voltage. This means it converts the energy generated by the system into a steady, sinusoidal AC voltage with a frequency of 50 Hz. This standardized form of electricity is what the grid requires to ensure the smooth and reliable operation of electrical devices and systems connected to it.

The six-switch inverter relies on a sophisticated control mechanism at its core, governed by PWM signals. Through precise modulation of the duty cycles of these signals, the inverter ensures accurate regulation of not only output voltage and frequency but also phase, thereby providing users with enhanced control and stability. This precise control mechanism enhances the converter's performance and reliability.

### 5.2.1 Circuit

In the figure below, we observe the MATLAB circuit and its associated components utilized for the converter responsible for grid connection.

### 5.2.2 Control

The converter incorporates active power and reactive power control, as it is paramount in generation systems to manage the electricity injected into the grid. Injecting excessive reactive power can lead to various perturbations in the grid. These perturbations include voltage fluctuations,

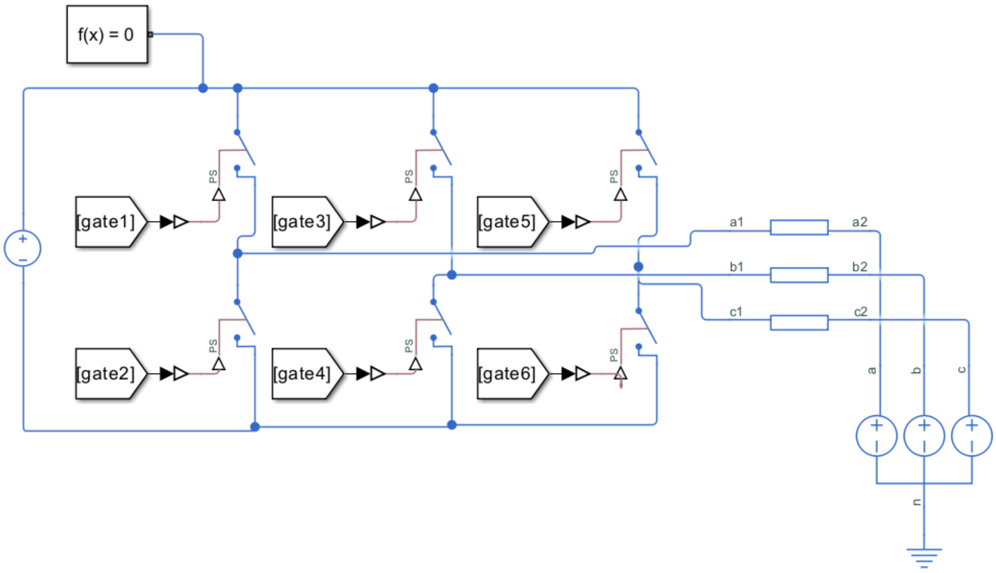


Figure 5.4: Grid converter.

increased transmission line losses, and compromised grid stability. Thus, precise control of both active and reactive power outputs is essential to ensure grid stability, efficient power transmission, and reliable operation of the entire electrical network.

The following equations can express the active and reactive power supplied to the grid:

$$P_a = \frac{3}{2} \times (v_{sd} \times i_{sd} + v_{sq} \times i_{sq}) \tag{5.1}$$

$$Q_{power} = \frac{3}{2} \times (-v_{sd} \times i_{sq} + v_{sq} \times i_{sd}) \tag{5.2}$$

In situations where connection to the grid is necessary, understanding the grid voltage phase is paramount to avoid perturbations and ensure stable operation. A Phase-Locked Loop (PLL) system is commonly employed to achieve this. The PLL system enables the estimation of the grid voltage's frequency and phase, providing crucial information for synchronization and control purposes.

By utilizing a PLL, we can align $\phi$ with the direct component of the voltage, such that $v_{sq} = 0$. Considering this equality to zero, it becomes possible to control the active and reactive power independently.

$$P_a = \frac{3}{2} \times v_{sd} \times i_{sd} \tag{5.3}$$

$$Q_{power} = -\frac{3}{2} \times v_{sd} \times i_{sq} \tag{5.4}$$

Developing in order of $i_{sd}$ and $i_{sq}$ we have:

$$i_{sd} = P_a \times \frac{2}{3} \times \frac{1}{v_{sd}} \tag{5.5}$$

$$i_{sq} = -Q_{power} \times \frac{2}{3} \times \frac{1}{v_{sd}} \tag{5.6}$$

After obtaining the reference currents, We can proceed with a conventional control method as shown in Figure 5.5.

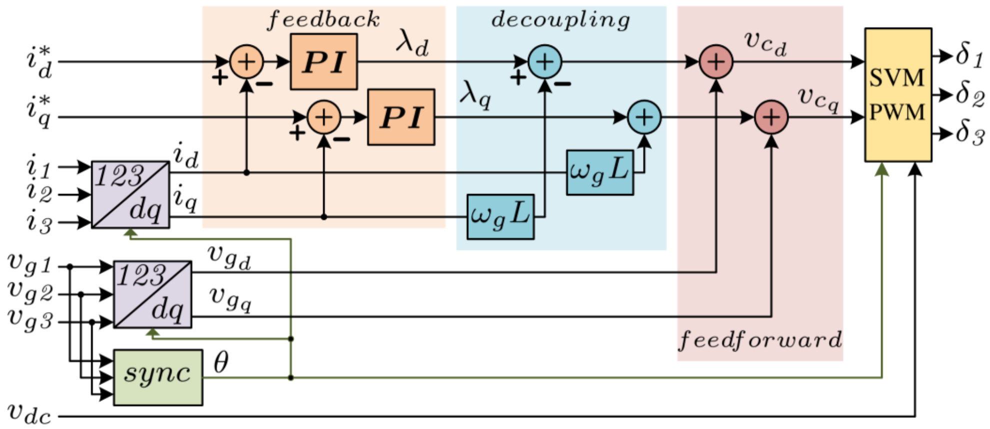


Figure 5.5: Conventional Control in a Three-Phase Converter [32].

### 5.2.3 Simulation

In Figure 5.6, a phase-locked loop is implemented in MATLAB using a block titled "Sinusoidal Measurement (PLL, Three-Phase)."

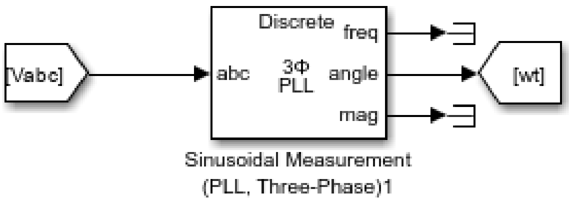


Figure 5.6: PLL.

Through Figures 5.7 and 5.8, we can observe the transformation process from three-phase voltages and currents to the reference frame dq0. These figures provide insight into how this conversion was achieved.

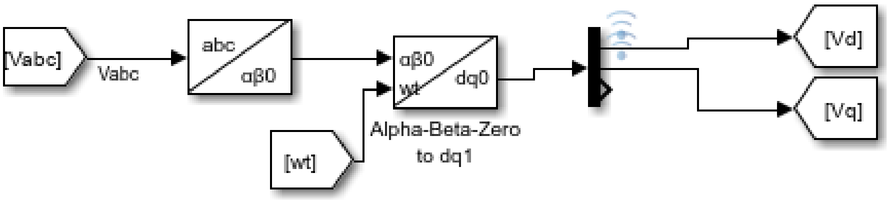


Figure 5.7: abc to dq0 Voltages.

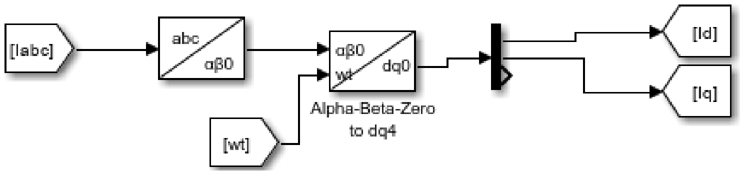


Figure 5.8: abc to dq0 Currents.

After establishing the voltage phase, along with the currents and voltages in the dq0 reference frame, the control of the converter can be implemented. This implementation is demonstrated in Figure 5.9.

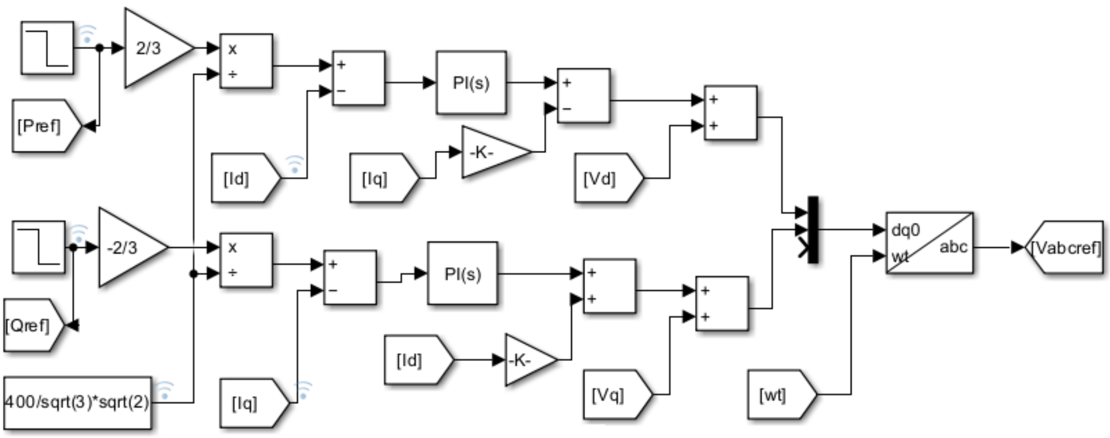


Figure 5.9: Grid converter control.

The complete scheme of the grid converter and the associated control can be seen in Appendix A.2.

The simulation of the grid converter was conducted with an active power of P = 3000 W and P = -3000 W from t = 0.4 s to t = 1.1 s. The reactive power was also set to Q = 750 VAR and Q = -500 VAR from t = 0.8 s to t = 1.1 s.

Analyzing Figure 5.10, it becomes evident that the converter tracks the reference for active power. However, some perturbations occur during reference variations, whether for active or reactive power.

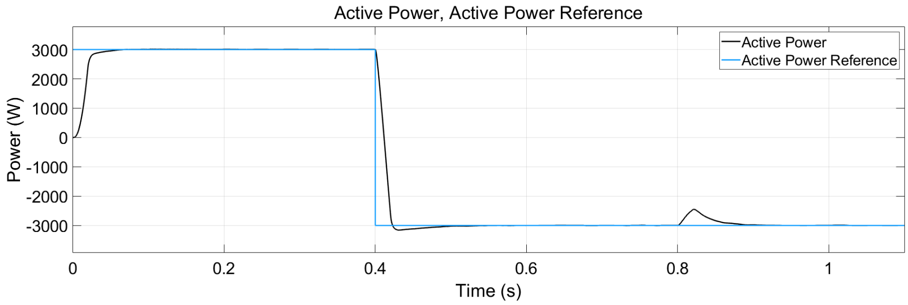


Figure 5.10: Active power compared to reference.

Upon observing Figure 5.11, it is evident that the reactive power also follows the reference, exhibiting a similarity to the behavior observed in active power tracking. However, perturbations occur during changes in the reference, albeit slightly larger in magnitude than those observed in active power tracking.

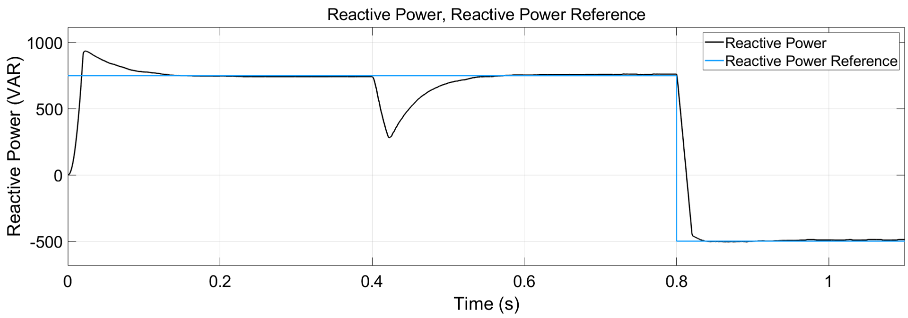


Figure 5.11: Reactive power compared to reference.

The currents and voltages shown in the figure below exhibit the expected behavior as their waveforms are sinusoidal.

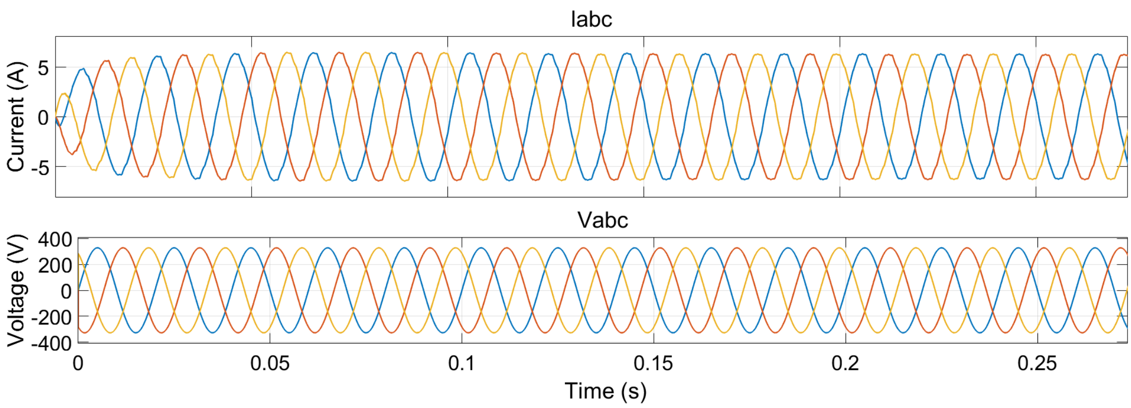


Figure 5.12: Grid currents and voltages.

## 5.3 Turbine and Generator

To facilitate energy production, it is imperative to harness the latent energy stored within water bodies effectively. This entails a meticulous process of transforming this potential energy first into mechanical energy and subsequently into electrical power. Integrating a water turbine and an induction motor proves to be indispensable to achieve this. The water turbine acts as the initial catalyst, capturing the kinetic energy inherent in flowing water and converting it into rotational mechanical energy. Subsequently, the induction motor plays a pivotal role in further transforming this mechanical energy into electricity, facilitating the efficient generation of renewable energy.

The water turbine is specifically designed to operate with the energy from flowing water. There are various types of turbines, such as propeller, Kaplan, Pelton, and Francis turbines, each suitable for different flow conditions and head heights. The correct turbine choice depends on several factors, including the volumetric flow rate and the available head height. For instance, Kaplan turbines are ideal for low-head, high-flow water streams, while Pelton turbines are more efficient in high-head, low-flow scenarios.

After the initial conversion of kinetic energy into mechanical energy, the induction motor comes into play. This type of motor is widely used due to its robustness and efficiency in converting mechanical energy into electrical energy. When the induction motor's shaft is driven by the turbine, the rotational movement generates a varying magnetic field within the motor. This magnetic field induces an electric current in the stator windings, resulting in the production of electricity.

Integrating these components efficiently ensures that the potential energy of water is maximized, resulting in a renewable energy generation system that is both efficient and sustainable. By optimizing each step of the process, from capturing the kinetic energy with the turbine to the final conversion into electricity by the induction motor, we can ensure the production of clean and reliable energy, significantly contributing to the reduction of dependence on non-renewable energy sources.

### 5.3.1 Turbine

Selecting the optimal turbine type was paramount and necessitated a thorough understanding of specific requirements, primarily revolving around power output, rotational speed, and head. Table 5.4 shows these parameters for this particular case.

Table 5.4: Turbine parameters

| Turbine parameters | |
|---|---|
| Speed (rpm) | 1000 |
| Power (W) | 4000 |
| Head (m) | 2 |

After obtaining the parameters, the software developed by Comillas Pontifical University was utilized. This software facilitated the selection of the turbine type, sizing its parameters, and estimating its efficiency yield. Subsequently, the results obtained will be meticulously verified to ensure rigor in the analysis.

The simulation yielded a propeller turbine, a variation of a Kaplan without blade angle regulation, and specific geometric, yield, and flow results for this turbine are presented in Table 5.5. A visual explanation of each variable represented in the table can be found in Figure 5.13.

The simulation yielded a propeller turbine, which is a variation of a Kaplan turbine without blade angle regulation. This result was anticipated because we are working with a small head and a large flow rate. Propeller turbines are particularly well-suited for these conditions. Specific geometric, yield, and flow results for this turbine are presented in Table 5.5. A visual explanation of each variable represented in the table can be found in Figure 5.13.

By utilizing a propeller turbine in this context, we can achieve a high efficiency of 88%, as indicated by the simulation results. This efficiency is largely due to the turbine's design, which is optimized for the specific flow and head conditions of the project.

Table 5.5: Simulation results

| $D_n$ | $D_a$ | B | Z (number of blades) | Efficiency (%) | Flow $(m^3/s)$ |
|---|---|---|---|---|---|
| 0.12 | 0.3 | 0.13 | 4 | 88 | 0.23 |

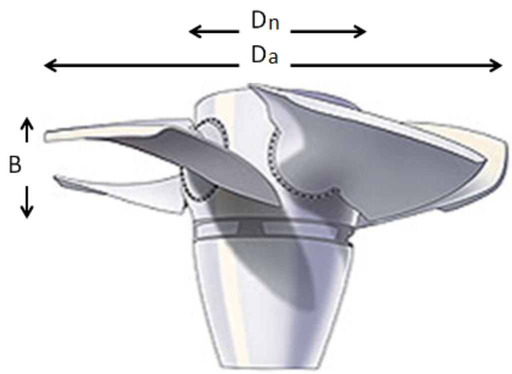


Figure 5.13: Propeller turbine [28].

The variable $\sigma$ denotes a pivotal characteristic factor crucial for sizing Kaplan turbines. It is intricately influenced by several key parameters, namely, the rotational speed of the turbine wheel, the volumetric flow rate, and the acceleration of gravity. This factor is a cornerstone in determining the Kaplan turbine's optimal specifications and dimensions. [33]

$$\sigma = \frac{2 \times n \times \sqrt{\pi \times Q}}{(2 \times g \times H)^{\frac{3}{4}}} \tag{5.7}$$

After scrutinizing Figure 5.14, deriving the value of $\delta$ from the previously calculated $\sigma$ is plausible. Additionally, upon closer examination of the exact figure, discerning the correlation between the outer and inner diameters of the runner blade is equally viable. Furthermore, the number of blades can also be determined.

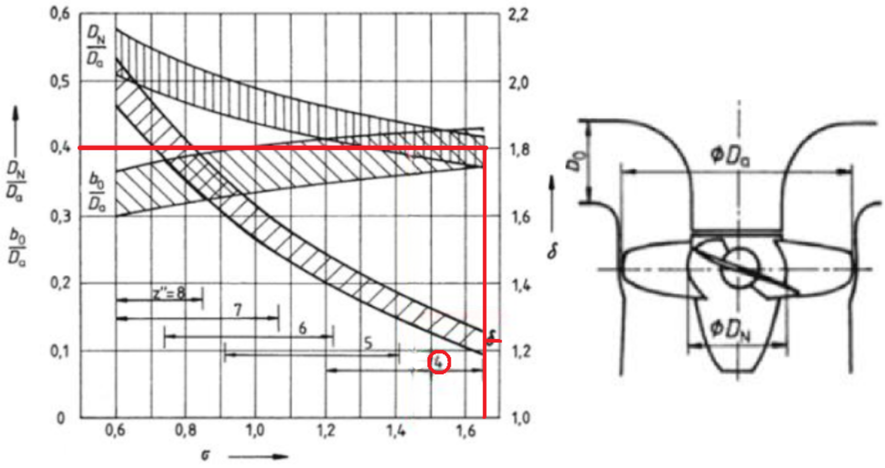


Figure 5.14: Design diagram for a Kaplan turbine [33].

$$D_a = \frac{2 \times \delta}{\sqrt{\pi}} \times \sqrt[4]{\frac{Q^2}{2 \times g \times H}} = 0.27m \tag{5.8}$$

$$D_N = D_a \times 0.4 = 0.11m \tag{5.9}$$

Table 5.6: Turbine sizing comparisons

| Method | D (m) | Di (m) | Z (number of blades) |
|---|---|---|---|
| Software | 0.30 | 0.12 | 4 |
| Sizing manually | 0.27 | 0.11 | 4 |

We can apply the same principle used in wind turbines to calculate the power generated by turbines. The formula for determining power output is expressed below:[34]

$$P = \frac{1}{2} \times \rho \times A \times V^3 \times C_p \tag{5.10}$$

$$A = \frac{\pi \times D^2}{4} \tag{5.11}$$

where:

- $\rho$ is the water density ($kg/m^3$);
- A is the projected area of the rotor ($m^2$);
- $C_p$, is a power coefficient;

- $v$ is water speed (m/s).

We can assume a coefficient of performance $C_p$ of 0.33 [34].

This formula enables us to estimate the turbine's powers, providing valuable insights into its performance.

The speed of water in the turbine runner was calculated using the Bernoulli equation. However, this calculation assumed that the pressure at both inlet and outlet points equals atmospheric pressure and neglected losses in the canal.

The expression of the Bernoulli equation is as follows:

$$P_1 + 0.5 \times \rho \times v_1^2 + \rho \times g \times z_1 = constant \tag{5.12}$$

Where:

- $P_1$, is the pressure of the fluid (Pa);
- $\rho$, is the density of the fluid ($kg/m^3$);
- $v_1$is the velocity of the fluid (m/s);
- g is the acceleration due to gravity ($m^2/s$);
- $z_1$, is the height of the fluid above a reference (m);

The demonstration to calculate the water speed using the Bernoulli equation at the turbine's inlet is determined by comparing the inlet and outlet of the canal.

$$P_1 + 0.5 \times \rho \times v_1^2 + \rho \times g \times z_1 = P_2 + 0.5 \times \rho \times v_2^2 + \rho \times g \times z_2 \tag{5.13}$$

Deducing the comparison above in order to $v_2$ is possible to obtain the equation 5.14.

$$v_2 = \sqrt{v_1^2 + 2 \times g \times h} \tag{5.14}$$

Table 5.7: Speed results in water canal

| $v_1$ (m/s) | $v_2$ (m/s) | $z_1$ (m) | $z_2$ (m) |
|---|---|---|---|
| 4.04 | 7.51 | 2 | 0 |

A MATLAB function has been developed to do the simulations. This function takes several parameters as input, including the diameter of the runner wheel, water flow rate, gravitational acceleration, $C_p$ coefficient, head, and water density. The output of this function is the mechanical power generated by the turbine; the inputs and outputs are depicted in Figure 5.15 and Figure 5.16 offers a detailed breakdown of the function's components.

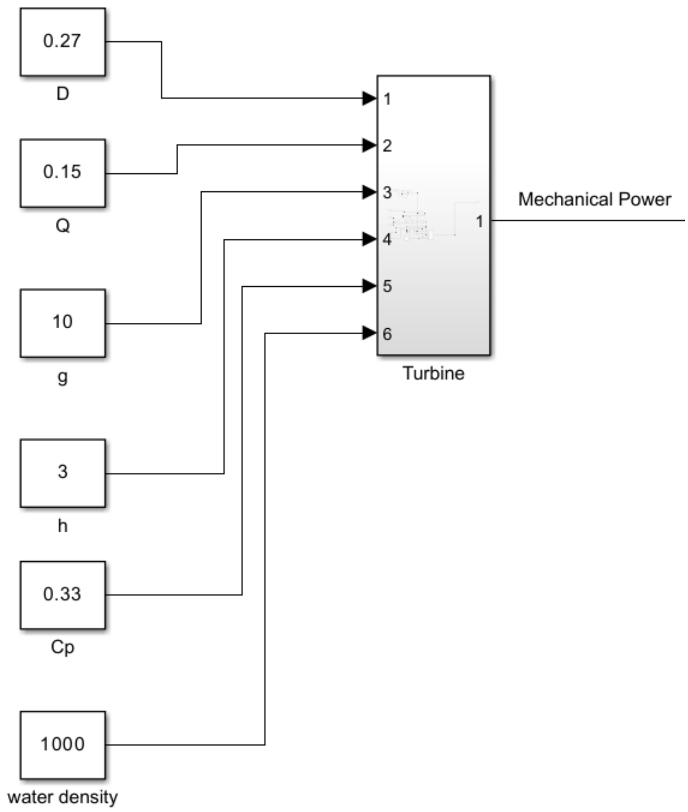


Figure 5.15: MATLAB function's inputs and outputs of the turbine model.

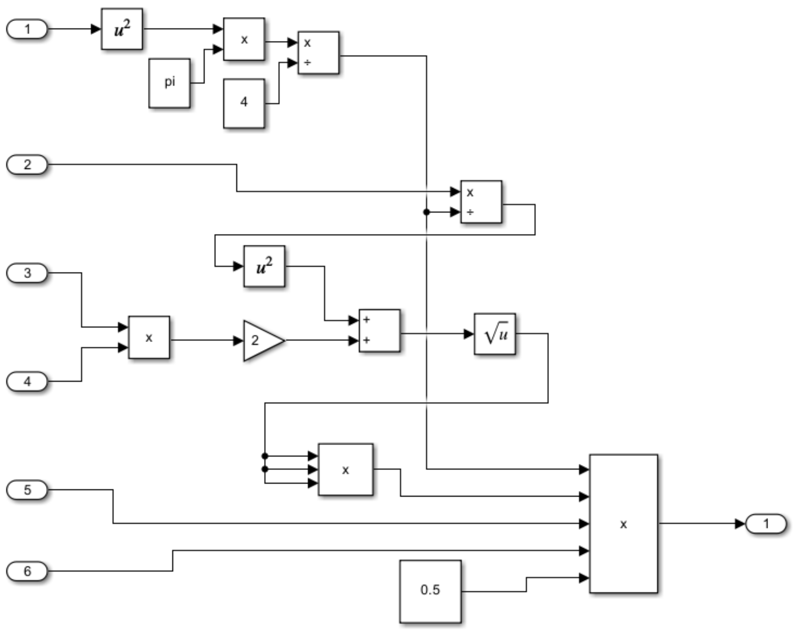


Figure 5.16: Detailed turbine model.

In Figure 5.17, the results indicate that under nominal turbine conditions, a mechanical power output of 3973 W was achieved, which closely aligns with the expected value of 4000W. The difference between the observed and predicted values could be attributed to the approximation used within the expression to calculate the power.

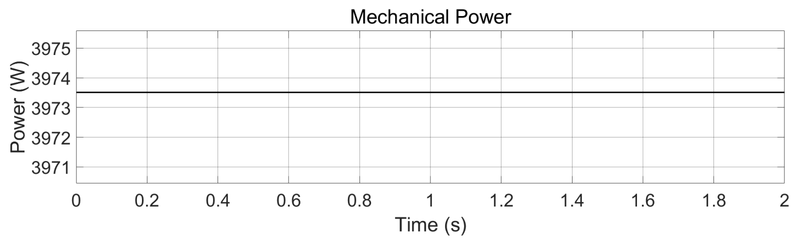


Figure 5.17: Turbine mechanical power.

### 5.3.2 Generator

The induction motor was chosen for this specific application due to its simplicity and cost-effectiveness, as it eliminates the need for additional excitation systems. This choice streamlines the setup and reduces costs while ensuring reliable operation.

Table 5.8: Induction motor [35]

| Power (kW) | Rated voltage (V) | Rated Current (A) | Speed (rpm) | Rated Frequency (Hz) |
|---|---|---|---|---|
| 4 | 400 | 9 | 960 | 50 |

Before commencing simulations with the motor, it is essential to determine its impedance values accurately. This is achieved by conducting the no-load and locked rotor tests.

During the no-load test, parameters such as steel losses, magnetization reactance, and inductance are estimated. The motor runs freely without any mechanical load attached to the shaft during this test. These parameters offer insights into the motor's performance under light or no load conditions.

The relationships derived during the no-load test are expressed mathematically as follows [36]:

$$\phi_o = \arccos \frac{P_o}{\sqrt{3} \times U_o \times I_o} \tag{5.15}$$

$$R_m = \frac{U_o^2}{P_{fer}} \tag{5.16}$$

$$X_m = \frac{\frac{U_o}{\sqrt{3}}}{I_o \times \sin(\phi_o)} \tag{5.17}$$

$$L_m = \frac{X_m}{2\pi f} \tag{5.18}$$

On the other hand, the locked rotor test helps determine parameters such as rotor resistance, stator leakage reactance, and rotor leakage reactance. This test involves mechanically blocking the rotor and applying a reduced voltage to the stator. These parameters are essential for evaluating the motor's performance under heavy load or starting conditions.

The relationships derived during the locked rotor test are expressed mathematically as follows[36]:

$$\phi_c = \arccos(\frac{P_c}{\sqrt{3} \times U_c \times I_n}) \tag{5.19}$$

$$I_{1c} = I_n \times (\cos(-\phi_c) + i\sin(-\phi_c)) \tag{5.20}$$

$$I_{oc} = \frac{\frac{U_c}{\sqrt{3}}}{\frac{R_m \times i \times X_m}{R_m + i \times X_m}} \tag{5.21}$$

$$I_{2c} = I_{1c} - I_{oc} \tag{5.22}$$

$$R_2 = \text{real}\left(\frac{\frac{U_c}{\sqrt{3}}}{I_{2c}}\right) - R_1 \tag{5.23}$$

$$X_r = \text{imag}\,\frac{\left(\frac{\frac{U_c}{\sqrt{3}}}{I_{2c}}\right)}{2} \tag{5.24}$$

$$X_s = X_r \tag{5.25}$$

By utilizing the data presented in Table 5.9 and 5.10, we can derive the motor resistances through specified relationships. The outcomes of these calculations are documented in Table 5.11.

Table 5.9: No load test [37]

| No load test | |
|---|---|
| $U_0$ | 401.3 |
| $I_0$ | 5.33 |
| $P_{cu}$ | 244.0 |
| $P_m$ | 26.9 |
| $P_{fe}$ | 125.4 |

Table 5.10: Locked-rotor test [37]

| Locked-rotor test | |
|---|---|
| U(V) | 386 |
| I(A) | 627.27 |
| $P_1$(kW) | 23.42 |

Table 5.11: Motor impedances

| Impedances | |
|---|---|
| $R_1$ | 0.9403 |
| $X_s$ | 1.5299 |
| $R_2$ | 1.3714 |
| $X_r$ | 1.5299 |
| $X_m$ | 43.5638 |

#### 5.3.2.1 Simulation

A scalar control was employed to control the motor. This method allows for speed manipulation by adjusting the curves of frequency and voltage. Figure 5.18 shows the implementation of this control in Simulink. First, the speed values are compared. The result is processed by a PI controller, after which the speed is converted into a frequency reference. The scalar control processes this frequency reference, obtaining the voltage references. Ultimately, the PWM generator obtains the gate signals.

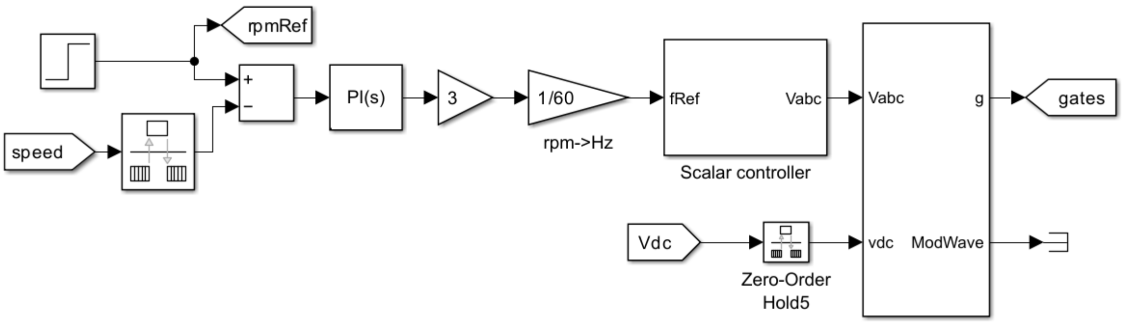


Figure 5.18: Generator scalar control.

In Figure 5.19, the complete system setup is illustrated. This setup includes the generator, inverter, DC bus, and an ideal source of torque that represents the turbine. For further analysis, it is possible to see the scheme in Appendix A.3.

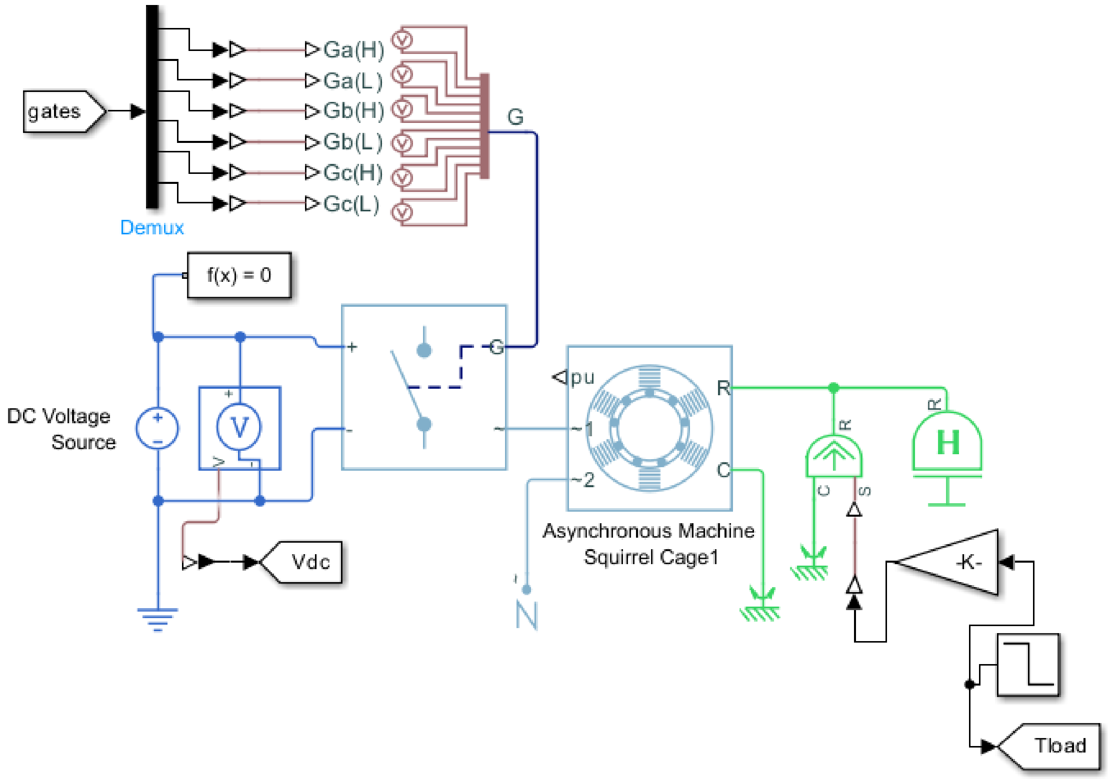


Figure 5.19: Generator Matlab circuit.

A simulation was conducted using the selected motor to test the implementation. In this simulation, the speed was set to 500 rpm during the first second and then increased to 1000 rpm. For the torque, -20 Nm was applied to the motor during the first two seconds, followed by -40 Nm.

In Figure 5.20, a comparison between the machine's electric torque and the turbine's load torque is presented. The machine torque tracks the turbine torque, exhibiting only perturbations when there are changes in the reference or generator speed.

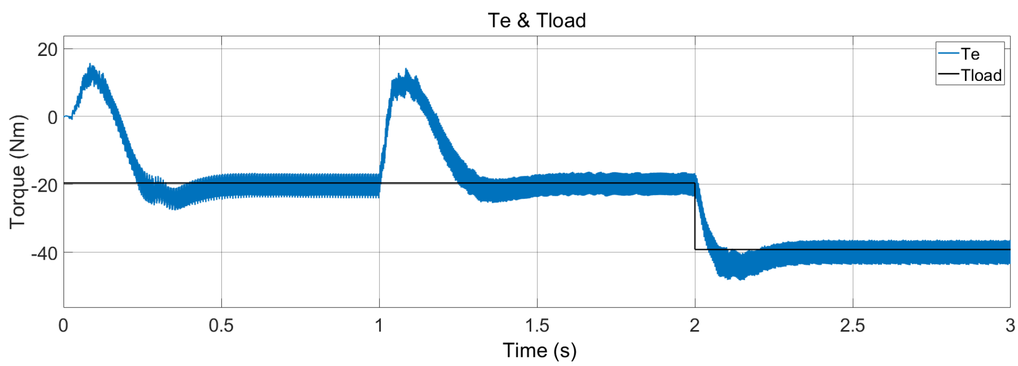


Figure 5.20: Generator torque.

The figure below displays the rotor speed and the rotor reference. It can be observed that the rotor speed follows the reference.

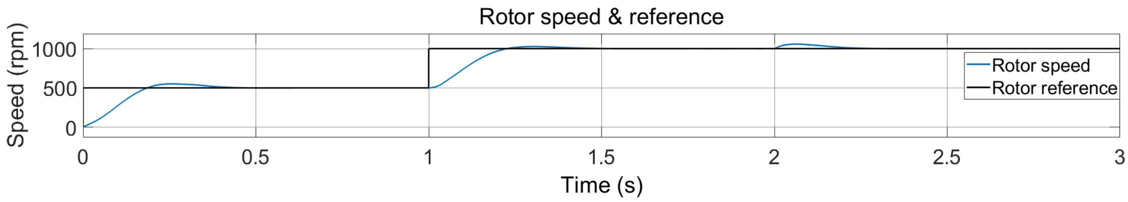


Figure 5.21: Generator speed vs reference.

In Figure 5.22, the power produced by the motor is presented. This power output is as expected: in the first second, the torque is 50% of the nominal value, so the potential power production is limited. However, the motor cannot produce the full available power because the speed is not at the nominal value. After the speed reaches 1000 rpm, with the torque at half the nominal value, the power output is 2000 W. When the torque reaches the nominal value, the power output increases to 4000 W.

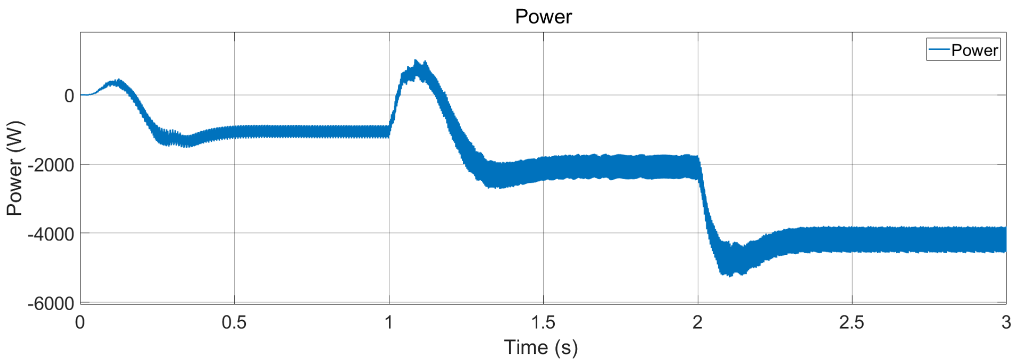


Figure 5.22: Generator active power.

## 5.4 Complementary System

Drought is a recurring issue in Portugal, particularly severe in some years. This problem is especially prevalent during the summer months. To mitigate the effects of drought, this section will explore alternative renewable energy sources, specifically wind and solar power. The analysis provided will be simplified and not exhaustive, focusing on the potential of these sources to supplement energy needs.

### 5.4.1 Solar power

Solar power is a green energy source that relies solely on the sun's energy. It can generate a significant amount of energy during the daytime, enough to power consumption needs and charge batteries for use at night.

Solar energy production can significantly reduce in winter due to shorter days and less intense sunlight. However, this is not critical in the proposed system because winter typically brings ample rainfall, allowing the hydroelectric system to compensate for the reduced solar output. This complementary relationship between solar and hydroelectric power ensures a reliable and sustainable energy supply throughout the year.

The KACO blueplanet PV-designer software was used to analyze the potential of a solar system. This software allows users to input the installation location, type of panels, and their positioning. It then calculates the power produced each month. Although the software can also incorporate load analysis, it was not considered for this study.

In figure 5.23, It is possible to observe the energy produced by installing a 4 kW solar system in Arcos de Valdevez. This location was chosen due to its proximity to the rivers, which serve as the foundation for this work. This analysis provides an estimate of the monthly energy output based on the specified location and system configuration,

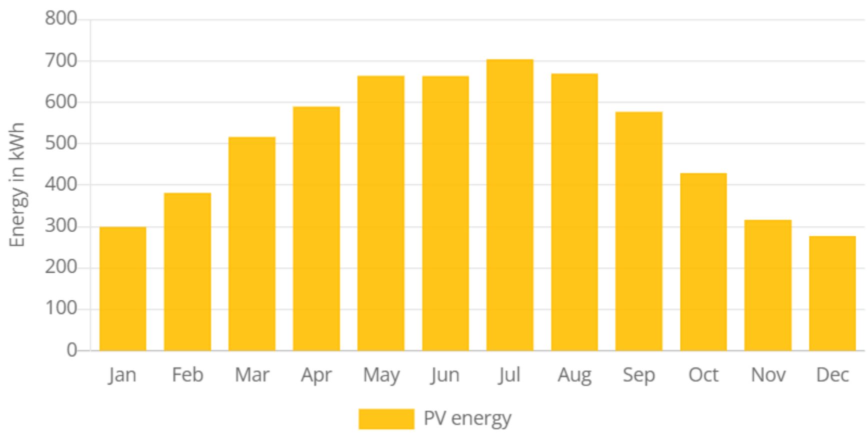


Figure 5.23: Energy produced in a 4 kW solar system calculated through Kaco [38].

Based on the load profile presented in Figure 4.1, it is possible to estimate the monthly load consumption.

$$Load_{month} = 556.92kWh \quad (5.26)$$

This solution can help address the problem of drought by ensuring a sufficient energy supply. As observed, the load values are lower than the power generation from the solar system during the months of April, May, June, July, and September. During these months, we assume the hydro generator generates no power.

Since the power generated by the 4 kW solar system covers the energy loads for five months without hydro generation, it appears to be oversized. Therefore, another simulation will be conducted with only 3 kW of solar power installed to match the energy demands better. This adjustment aims to optimize the system's efficiency and cost-effectiveness.

Observing figure 5.24, it is evident that a 3 kW solar system can supply almost all energy loads in July and August.

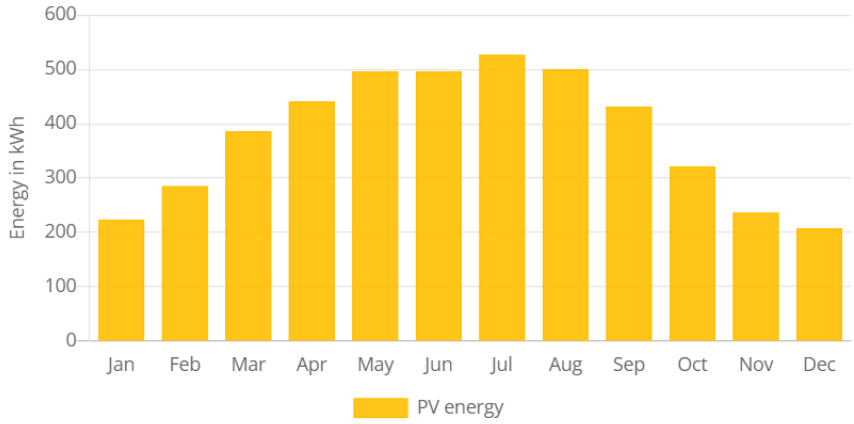


Figure 5.24: Energy produced in a 3 kW solar system calculated through Kaco [38].

The choice of power capacity for the solar system to install will depend on the expected level of drought and the predicted power generation from the hydro system.

### 5.4.2 Wind power

Wind power is a green energy source that harnesses the energy of the wind. It can generate a significant amount of energy when wind conditions are favorable.

Wind energy production can vary depending on the season and local weather patterns. This section will study whether a wind generator can support the system during months with lower water availability, ensuring a stable and sustainable energy supply even when hydroelectric output is reduced.

A study was conducted on the historical wind data in Arcos de Valdevez to assess the wind potential. The results are presented in Table 5.12.

Table 5.12: Average wind values in August in Arcos de Valdevez[39]

| Year | Average wind (km/h) |
|---|---|
| 2010 | 15.0 |
| 2011 | 12.37 |
| 2012 | 12.67 |
| 2013 | 14.96 |
| 2014 | 12.23 |
| 2015 | 13.92 |
| 2016 | 15.33 |
| 2017 | 15.33 |
| 2018 | 15.7 |
| 2019 | 14.15 |
| 2020 | 15.26 |

After obtaining the wind values, it is possible to calculate the monthly wind energy production. A 3 kW wind turbine was selected, and the rotor area was retrieved.

Using the wind data in the table above, it was possible to determine the average wind speed.

$$W_{average} = 14.26km/h \tag{5.27}$$

A wind power calculator obtained a potential wind power output of 192 Wh for the specified conditions. [40][41]

$$W_{production} = 24 \times 192 = 4.608\text{kWh per day} \tag{5.28}$$

$$W_{production} = 30 \times 4.608 = 138.240\text{kWh per month} \tag{5.29}$$

It obtained an average production of 138 kWh in August. This output is significantly lower than the expected energy loads, covering less than 30% of the required demand.

### 5.4.3 Conclusion

Choosing between solar and wind power seems easy if we only consider potential energy production. Solar power, for the same installed capacity, has the potential to produce more than three times the energy of a wind turbine. However, the decision might be different in areas with stronger wind conditions or where there is no suitable space to install solar panels.

## 5.5 Selected Products

In a project, it is very important to follow the theoretical analysis with a careful selection of components for building the project. In the following section, it is present possible components that can be used to construct the hydroelectric power station.

### 5.5.1 Turbine and Generator

Finding an exact match for the turbine needed for the project was a bit challenging. The simulations used a turbine with a nominal power of 4 kW. However, the most similar turbine available was selected since an exact match could not be found. This turbine, shown in Figure 5.25, has a cost of approximately 1763€ and a nominal power of 5 kW [42].

In an ideal scenario, the best approach would be to conduct a full sizing and design of the turbine. This would ensure that it could be specified a turbine that is perfectly suited to the project's specific requirements. After completing the design, it could be possible to collaborate with a company capable of manufacturing the custom turbine to meet the needs searched.

Figure 5.25: Kaplan turbine [42].

The chosen motor for this project is a 6-pole, 4 kW induction motor with a rotational speed of 960 rpm and a cost of 532€, and it is possible to observe it below[35].

Figure 5.26: Induction motor [35].

### 5.5.2 Converters

Unfortunately, it was not possible to find converters suitable for this application. Therefore, in the case of implementation, the best approach is to build all of them from scratch.

### 5.5.3 Battery

The battery chosen for the power station is the SOLARX-PRO-795B6. These batteries have a capacity of 9.5 kWh, require no maintenance, and cost 2000€. They are represented in Figure 5.27 [43].


Figure 5.27: Batteries [43].

# Chapter 6

# Final conclusions and future work

## 6.1 Conclusions

The development of this micro-hydroelectric project necessitates various analyses and the refinement of crucial components such as turbines, generators and converters. Among these tasks, the simulation that integrates these elements poses a significant challenge, often being the stage where complexities arise.

The advancement of this micro-hydroelectric system presents several notable contributions. Firstly, it is a renewable energy source, harnessing sustainable power from the natural water flow. Additionally, it fosters local development by creating job opportunities in constructing and maintaining the micro-hydroelectric system. Furthermore, its capability to extend electricity access to remote or rural areas lacking such access is a significant societal benefit.

In the second chapter, a study was conducted to understand the technology developed in this field and the main components needed to build a micro-hydroelectric system. This chapter also included a cost analysis of these elements.

Thirdly, it was a moment to analyze two projects that are similar to the intended project. In this chapter, it was the main objective to see if there could be potential to improve the work that was being developed.

Moving to the fourth chapter, it was presented higher-level simulations, demonstrating the feasibility of controlling a battery system under various operational conditions.

Lastly, in the fifth chapter, a detailed analysis was performed to develop all essential elements of a micro-hydroelectric plant as well as to implement its control systems. This chapter also explored potential improvements, such as integrating solar panels or wind turbines. Additionally, some products were chosen for the project. Even though these are the selected products, there are other options on the market that could also perform well in their respective functions.

This work successfully designed a hydropower station, considering all components and ensuring that none were overlooked. Additionally, a high-level control system was developed. Through all simulations, it was established that integration of all components is feasible. It is also important to mention that for those, it was considered a perfect environment as well as conditions.

This study is of great value to individuals interested in green energy and to outline the climate changes. In addition to that, it provides a potential solution for people who currently lack access to electricity. Although this study was aimed at being comprehensive, time constraints prevented the detailed sizing and analysis of all components.

This study contributes to developing a type of energy production with a significant history in Portugal, now adapted to a smaller scale of power that allows for widespread implementation.

## 6.2 Satisfaction of Objectives

The objectives defined for this dissertation were successfully met. A study was conducted on the requirements and operation of the turbines, a characterization of all subsystems, a simulation of the subsystems, and their sizing. Finally, an analysis was performed to enhance the system.

Ultimately, developing a solution capable of producing energy efficiently was possible. This solution is designed to be integrated seamlessly, functioning like a plug-and-play solution. It must only be placed in a river with the appropriate conditions, and all the necessary components to generate energy are included.

## 6.3 Future work

In the future, it would be beneficial for further research to simulate all components together and to build a physical model of this solution.

Additionally, a more in-depth study on using complementary energy sources would be valuable. This includes determining the most suitable complementary energy source and subsequently simulating its integration.

In an ideal scenario, it would be advantageous to develop a customized system. Selecting from a predefined portfolio of turbines and complementary energy sources would be possible depending on the specific location. For example, having Pelton and Kaplan turbines available would allow for integration in locations with either high or low head heights. Similarly, choosing between a wind turbine and solar panels as complementary energy sources would enhance the system's adaptability and efficiency.

# Bibliography

[1] APREN, *Energias renováveis - produção*, https://www.apren.pt/pt/energias-renovaveis/producao, Viewed on 22 October 2023.

[2] R. M. Castro, *Energias Renováveis e Produção Descentralizada: Introdução à Energia Mini-Hídrica*. Universidade Técnica de Lisboa, Instituto Superior Técnico, DEEC / Secção de Energia, 2002.

[3] T. B. H. Association, *A guide to uk mini-hydro developments v3.0*, 2023. [Online]. Available: https://www.british-hydro.org/wp-content/uploads/2018/03/A-Guide-to-UK-mini-hydro-development-v3.pdf.

[4] J. Fritz, *Small and Mini Hydropower Systems*. New York: McGraw Hill, 1984.

[5] H. Ramos, A. B. de Almeida, M. M. Portela, and H. P. de Almeida, *Guideline for Design of SMALL HYDROPOWER PLANTS*. Belfast, North Ireland: WREAN and DED, 2000.

[6] D. P. N. Gomez, "Dimensionamento de uma pequena hídrica por via do aproveitamento e transformação de moinhos," Thesis, Universidade do Porto, 2016.

[7] A. Abbas, M. Alam, and R. Kumar, "Analytical analysis of combined effect of interior guide tube and draft tube on cross flow turbine performance," *Materials Today: Proceedings*, vol. 46, pp. 5372–5377, 2021, International Conference on Innovations in Clean Energy Technologies (ICET2020), ISSN: 2214-7853. DOI: 10.1016/j.matpr.2020.08.796. [Online]. Available: https://www.sciencedirect.com/science/article/pii/S2214785320366864.

[8] Y. Asaff, L. Oliveira, and V. De Negri, *Applicability of servo-pneumatic positioning systems for high loads*, Sep. 2008.

[9] S. K. Singal, V. Goel, H. Nautiyal, and D. E. Papantonis, "Chapter 5 - elements of small hydropower: Mechanical equipment," in *Small Hydropower*, S. K. Singal, V. Goel, H. Nautiyal, and D. E. Papantonis, Eds., Elsevier, 2023, pp. 71–152, ISBN: 978-0-323-91757-5. DOI: https://doi.org/10.1016/B978-0-323-91757-5.00006-3. [Online]. Available: https://www.sciencedirect.com/science/article/pii/B9780323917575000063.

[10] V. J. De Paris, "Projeto e simulação de um sistema de microgeração híbrido alimentado por energia hídrica e solar fotovoltaica," M.S. thesis, Universidade Federal de Santa Catarina, Centro Tecnológico, Programa de Pós-Graduação em Engenharia Elétrica, Florianópolis, 2022.

[11] S. J. Chapman, *Electric Machinery Fundamentals*, 5th. New York, NY: McGraw-Hill, 2012.

[12] American Journal of Engineering Research (AJER), "Micro hydro-electric energy generation-an overview," *American Journal of Engineering Research (AJER)*, vol. 6, no. 2, pp. 05–12, 2017.

[13] X. F. d. Silva, "Transformador eletrónico. princípios de funcionamento e controlo," M.S. thesis, Faculdade de Engenharia da Universidade do Porto, Jul. 2019. [Online]. Available: https://repositorio-aberto.up.pt/bitstream/10216/122032/2/348229.pdf.

[14] J. W. Kolar, T. Friedli, J. Rodriguez, and P. W. Wheeler, "Review of three-phase pwm ac–ac converter topologies," *IEEE Transactions on Industrial Electronics*, vol. 58, no. 11, pp. 4988–5006, 2011. DOI: 10.1109/TIE.2011.2159353.

[15] C. Klumpner and C. Pitic, "Hybrid matrix converter topologies: An exploration of benefits," in *2008 IEEE Power Electronics Specialists Conference*, 2008, pp. 2–8. DOI: 10.1109/PESC.2008.4591887.

[16] M. Y. Lee, "Three-level neutral-point-clamped matrix converter topology," Thesis, University of Nottingham, 2009.

[17] H. Chen, T. N. Cong, W. Yang, C. Tan, Y. Li, and Y. Ding, "Progress in electrical energy storage system: A critical review," *Progress in Natural Science*, vol. 19, no. 3, pp. 291–312, 2009, ISSN: 1002-0071. DOI: https://doi.org/10.1016/j.pnsc.2008.07.014. [Online]. Available: https://www.sciencedirect.com/science/article/pii/S100200710800381X.

[18] *1000 w micro hydro generator water turbine 220v hydroelectric power station*, https://www.ebay.com/itm/403937567555, Viewed on 5 January 2024.

[19] Ebay, *3 kw kaplan turbine hydro generator for river 220v ac single phase water turbines*, https://www.ebay.com/itm/235016520969, Viewed on 5 January 2024.

[20] Ebay, *3000 w hydropower generator 220v pulse hydro pelton turbine power generator*, https://www.ebay.com/itm/235070844045, Viewed on 5 January 2024.

[21] Adajusa, *Motor trifásico 22kw/3cv 230/400v 750 rpm*, https://adajusa.pt/pt/motores-eletricos-trifasicos-750-rpm-flange-b5-carcaca-de-aluminio/811-motor-trifasico-22kw-3cv-230-400v-750-rpm-b5-flange-carcaca-de-aluminio-8435532808114.html, Viewed on 5 January 2024.

[22] Adajusa, *Three-phase motor 4 kw 5.5cv 230/400v 1000 rpm ie1 flange b5*, https://adajusa.pt/pt/motores-eletricos-trifasicos-1000-rpm-flange-b5-carcacas-de-aluminio-ie1-ie2-ie3/801-motor-trifasico-4kw-55cv-230-400v-1000-rpm-ie1-flange-b5-8435532808015.html, Viewed on 5 January 2024.

[23] Efectoled, *Pylontech 48v h48074 lithium battery 3.6 kwh high voltage requires bms*, https://www.efectoled.com/pt/comprar-baterias/93817-bateria-de-litio-pylontech-48v-h48074-36-kwh-alto-voltaje.html, Viewed on 5 January 2024.

[24] Efectoled, *Huawei 360v luna2000 lithium battery module 5 kwh requires bms*, https://shorturl.at/vyDIU, Viewed on 5 January 2024.

[25] Tesla, *Powerwall*, https://www.tesla.com/pt_PT/powerwall/get, Viewed on 5 January 2024.

[26] Mouser, *Pf1000a-360*, https://shorturl.at/hjkCS, Viewed on 5 January 2024.

[27] Mouser, *Aops1500-24*, https://shorturl.at/dvVX5, Viewed on 5 January 2024.

[28] R. Palacios, *Simulador de turbinas*, https://pascua.iit.comillas.edu/palacios/fluidos/submenudiseno.html, Viewed on 7 January 2024, 2023.

[29] B. E. C. LLC, *Cross flow turbine design calculator*, https://shorturl.at/suF56, Viewed on 7 November 2024, 2023.

[30] Texas Instruments, *Basic calculation of a boost converter's power stage*, Application Note, Accessed on: April 16, 2024, 2022. [Online]. Available: https://www.ti.com/lit/slva372.

[31] Texas Instruments, *Basic calculation of a buck converter's power stage*, Application Note, Accessed on: April 16, 2024, 2015. [Online]. Available: https://www.ti.com/lit/an/slva477b/slva477b.pdf?ts=1713233314140&ref_url=https%253A%252F%252Fduckduckgo.com%252F.

[32] C. Ramos and A. Martins, "Polynomial current controller for a three-phase vsc connected to grid," in *IECON 2019 - 45th Annual Conference of the IEEE Industrial Electronics Society*, vol. 1, 2019, pp. 1956–1961. DOI: 10.1109/IECON.2019.8926745.

[33] C. Abeykoon and T. Hantsch, "Design and analysis of a kaplan turbine runner wheel," Jun. 2017. DOI: 10.11159/htff17.151.

[34] J. Faria, E. Margato, and M. J. Resende, "Self-excited induction generator for micro-hydro plants using water current turbines type," in *INTELEC 05 - Twenty-Seventh International Telecommunications Conference*, 2005, pp. 107–112. DOI: 10.1109/INTLEC.2005.335203.

[35] *6 Poles 4kW (5.5HP) 935RPM Shaft 38mm Electric Motor Three Phase 415V/720V*, https://cononmotor.com.au/product/6-poles-4kw-5-5hp-935rpm-shaft-38mm-electric-motor-three-phase-415v720v/, Viewed on 25 April 2024.

[36] A. C. A.
bibinitperiod C. Lda, *Projeto VEP – Veículo Eléctrico de Proximidade*, Viewed on 25 April 2024. [Online]. Available: https://web.fe.up.pt/~ee01086/vep/actas/doc1.pdf.

[37] C. Motor, *IE3-132M1-6*, https://cononmotor.com.au/wp-content/uploads/2022/05/IE3-132M1-6.pdf, Viewed on 25 April 2024, 2022.

[38] V. Software, *Kaco blueplanet pv-designer*, https://kaco-pvsol.valentin-software.com/, Viewed on 18 May 2024, 2024.

[39] Weather and Climate, *Weather in august 2020 in arcos de valdevez, portugal*, Viewed on 18 May 2024, 2020. [Online]. Available: https://weatherandclimate.com/portugal/viana-do-castelo/arcos-de-valdevez/august-2020#t2.

[40] Rechneronline, *Wind power calculator*, Viewed on 19 May 2024, 2024. [Online]. Available: https://rechneronline.de/wind-power/.

[41] D. Solar, *Aerogenerador bornay 3kw wind 25,2+*, Viewed on 19 May 2024, 2024. [Online]. Available: https://www.damiasolar.com/pt/aerogeradores/aerogenerador-bornay-3kw-wind-252.html.

[42] Ebay, *5kw 3 phase 400v axial flow turbine water wheel generator kaplan hydroelectric*, https://www.ebay.com/itm/235533457883, Viewed on 17 June 2024.

[43] Leroy Merlin, *Banco de baterias solarx pro 795b6 xunzel 12v 795ah 9.5kwh sem manutenção*, https://www.leroymerlin.pt/produtos/energias-renovaveis/baterias-e-carregadores-solares/banco-de-baterias-solarx-pro-795b6-xunzel-12v-795ah-9-5kwh-sem-manutencao-81989697.html, Viewed on 17 June 2024.

# Appendix A

# Appendix

## A.1 Buck-Boost

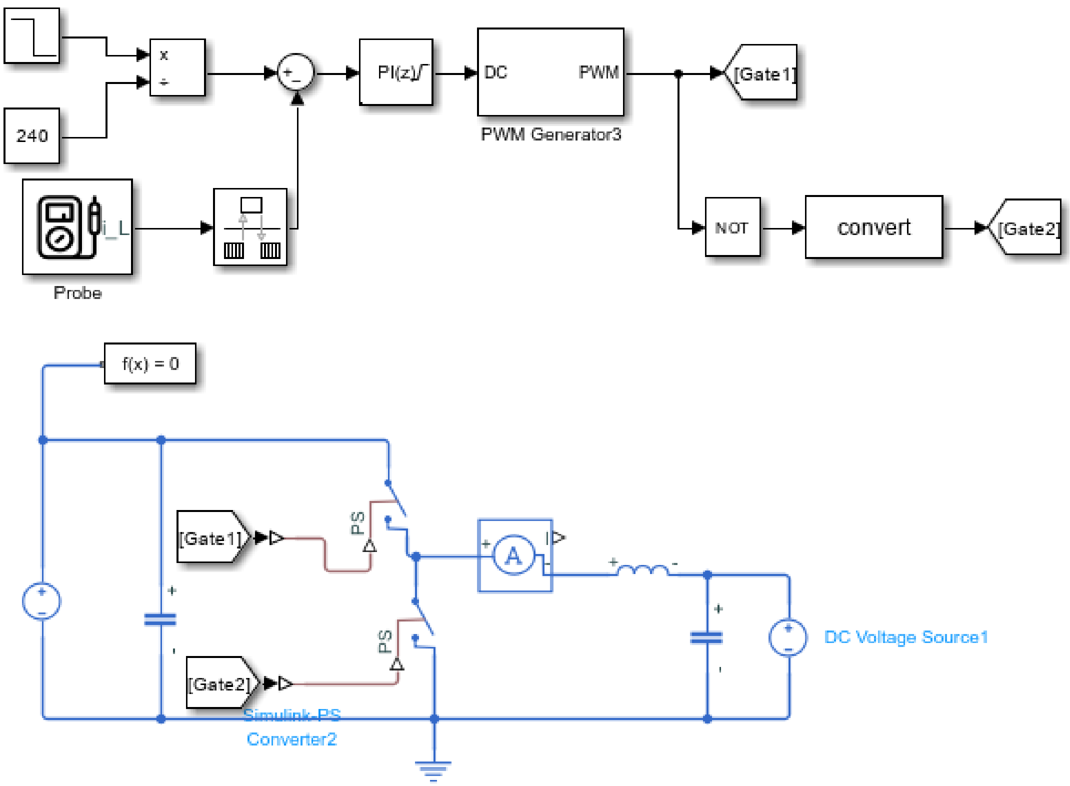

## A.2 Grid Converter

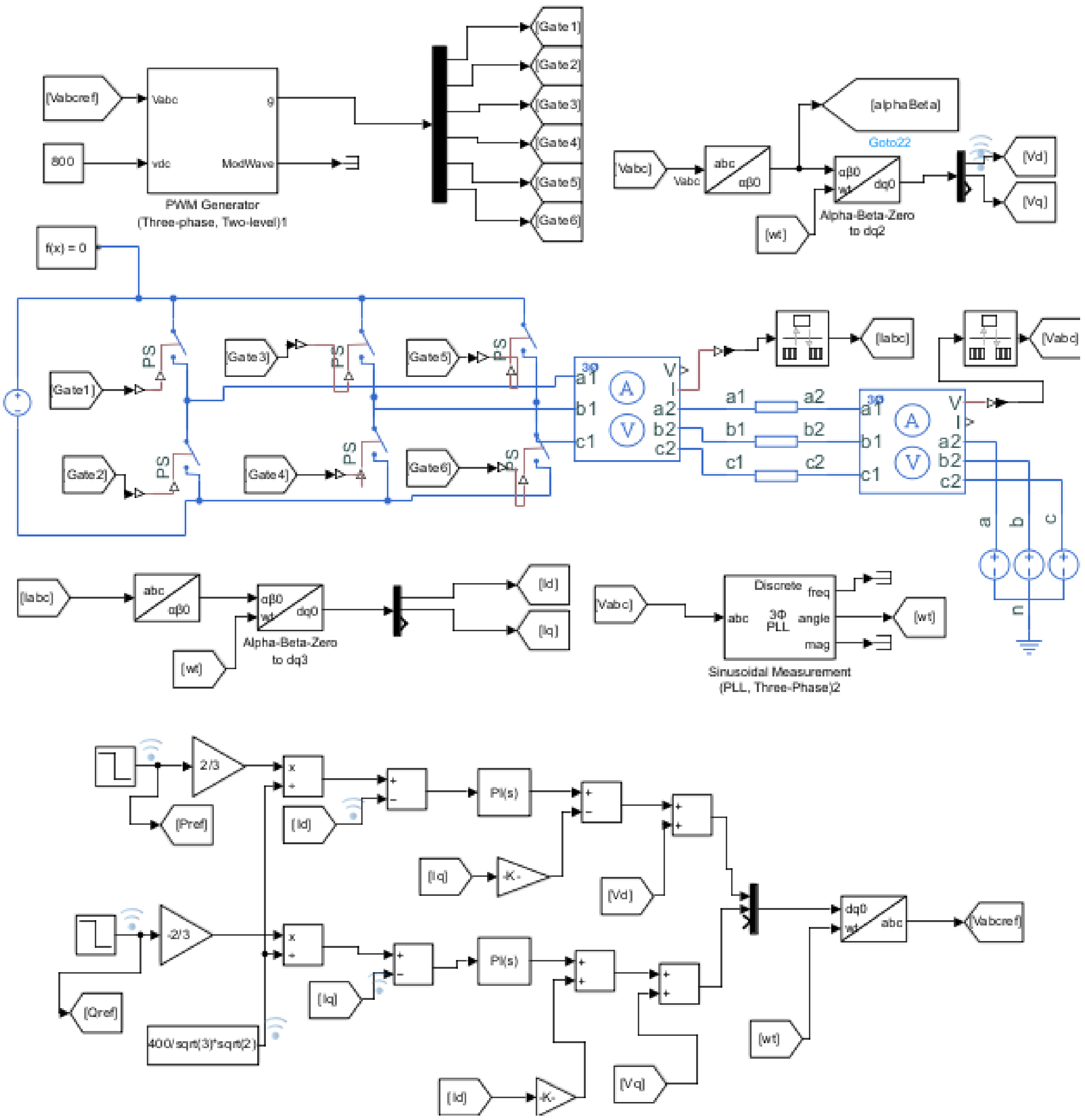

## A.3 Generator